Development of New CFT Column-CFT Beam Frame Structure using Self-compacting Concrete

Wang Ying

A dissertation submitted to
Kochi University of Technology
in partial fulfillment of the requirements
for the degree of

Doctor of Philosophy

Graduate School of Engineering
Kochi University of Technology
Kochi, Japan

March 2006

Development of New CFT Column-CFT Beam Frame Structure using Self-compacting Concrete

Wang Ying

Development of New CFT Column-CFT Beam Frame Structure using Self-compacting Concrete

Wang Ying

A dissertation submitted to
Kochi University of Technology
in partial fulfillment of the requirements
for the degree of

Doctor of Philosophy

Special Course for International Students
Department of Engineering
Graduate School of Engineering
Kochi University of Technology
Kochi, Japan

March 2006

Abstract

Concrete-filled steel Tube (CFT) is a kind of composite structure, in which concrete is cast into the steel tube. CFT structure combines steel and concrete in one member, which results in a member that has the beneficial qualities of both materials.

Almost all extensive research works and practical applications, however, have been limited to CFT column-steel beam systems nowadays. No research work and practical application were done on CFT column-CFT beam systems until now. The employment of CFT beam can improve the stiffness of whole building, delay the local buckling of beam and improve fireproof performance of the building.

Conventional concrete is able to be employed to make CFT column, whereas, it is impossible to be employed to construct CFT beam, due to the need of vibrating compaction work. This is a main obstacle for the application of CFT structure to beams. In order to apply CFT structure to beam, thus construct CFT column-CFT beam frame structure, self-compacting concrete (SCC) was introduced in this research. SCC has the advantage of being able to be compacted into every corner of a formwork purely by means of its own weight without the need of vibrating compaction.

The objective of this research was to develop a new CFT Column-CFT beam frame Structure using Self-compacting Concrete. Focus of this study was divided into the following three parts.

In the first part of the research, firstly, different connection details were designed; experimental work had been done in order to investigate the feasibility of employing SCC to CFT column-CFT beam structure and seismic behaviour of this new structure. Furthermore, in order to assess the strength, ductility and stiffness of the new CFT structure, four specimens, three CFT column-CFT beam connections and one hollow steel column-I beam connection, were made and tested. The introduction of a conventional steel specimen enables comparison with the new CFT structure. The experimental result shows that SCC can be successfully compacted into beam tube, and the new CFT structure connections provided adequate seismic behaviour.

In the second part of the research, a new concrete construction method for this new CFT column-CFT beam frame structure was described. According to the structural characteristics of this new frame structure, a new bottom up pumping method, different from the existing method which used for CFT column system, was developed. In order to assess the possibility of this new developed construction method, scale column-beam

subassembly using plastic plate was made and visual model of fresh concrete experiment was done. The result showed that the concrete model was able to be successfully cast into the subassembly which indicated that the new developed bottom up pumping method is possible to be practiced in the real building.

In the third part of the research, in order to validate the cost performance of this new CFT column-CFT beam structure, designs were carried out for building frames using both the new CFT structure and conventional steel structure. The amount of consumed materials and cost estimations of each designed new CFT and conventional steel building frame, were analysed and compared. The results showed that the new CFT column-CFT beam structure is able to exhibit high cost performance than pure steel structure.

Table of Contents

CHAPTER 1

INTRODUCTION

1.2 Background

Concrete-filled steel Tube (CFT) is a kind of composite structure, in which concrete is cast into the steel tube.

Depending on different cross sections, it can be divided into circular CFT structure, rectangle (square) CFT structure and polygon CFT structure, which are shown in Fig1.1. Since 1970, extensive investigations have verified that framing systems consisting of CFT columns and H-shaped beams have more benefits than ordinary reinforced concrete and steel systems, and as a result, in the building construction industry, concrete-filled tube (CFT) columns are gaining popularity all over the world.

1.2.1 Advantages of CFT Structure

Steel members have the advantage of high tensile strength and ductility. Concrete members have the advantages of high compressive strength and stiffness. Composite members combine steel and concrete in one member resulting in a member that has the beneficial qualities of both materials.

Compared with ordinary steel or reinforced concrete structure, the advantages of CFT structure are listed as the following:

Interaction between steel tube and concrete:

1) The occurrence of the local buckling of the steel tube is delayed, and the strength deterioration after the local buckling is moderated, both due to the restraining effect of concrete.
2) The strength of concrete is increased due to the confining effect provided form the steel tube, and the strength deterioration is not very severe, since the concrete spalling is prevented by the tube.

Cross-sectional properties:

3) The steel ratio in the CFT cross section is much larger than those in the reinforced concrete and concrete-encased steel cross sections.
4) The placement of the longitudinal steel at the perimeter of the section is the most efficient use of the material since it provides the highest contribution of the steel to section moment of inertia and flexural capacity.

Construction efficiency:

5) The steel tube serves as a form for casting concrete; no other reinforcement is needed since the tube acts as longitudinal and lateral reinforcement for the concrete core; concrete casting is done by tremie tube or bottom-up pumping method and these lead to saving of manpower and constructional cost and time.
6) Constructional site remains clean.

Fire resistance:

7) Concrete improves the fire resistance performance, and the amount of fireproof material can be reduced or its use can be omitted.

Cost performance:

8) The economy of a structure is usually enhanced if prefabricated units can be utilized, thereby reducing labor costs. In addition prefabricated units tend to be of higher quality. For buildings using CFT column system, the prefabricated units is accomplished by prefabricating in the certain heights of column segments with short beam stubs connected to the column using the selected connection detail. This "tree column" is then transported to the field and stacked on top of other segments. Floor beams are then spliced to the stub portion of the "tree column" and concrete is pumped into the hollow steel tubes. Such a concept schematically is shown in figure 1.2.

   Because of the advantages listed above, a better cost performance is obtained by replacing a steel structure by a CFT structure.

Ecology:

9) Environmental burden can be reduced by omitting the formwork, and by reusing steel tubes and high-quality concrete as recycled aggregates.

1.2.2 Research for CFT Column System

The CFT system was actively studied by construction companies as well as by the academia since around 1985. Design and construction methods were developed utilizing the findings of the studies, and the construction of CFT buildings increased after 1990.
In order to investigate the cost performance of CFT column system, some comparison research works had been done between CFT column system structure and steel system structure.

Ricles et al. (1995) demonstrated the superiority of CFT column system construction by designing a 20-story prototype building using two difference alternatives. The first system used wide flange (WF) columns, while the second system used CFT columns. A comparison of the two designs indicated that although the total weight of the CFT column system is 81% greater than that of the WF column system due to additional weight of concrete, the former has a total structural steel weight that is 22% less than the later. The reduced weight of steel in the CFT column system results in an overall cost reduction.

Shosuke Morino et al. (2001) investigated the cost performance of CFT column system by designed theme structures with 10, 24 and 40-story unbraced building frames made of CFT or Steel systems. CFT or steel is used for columns and H-shaped steel is used for beams. The results showed that the steel amount of CFT column is less by about 25% than that of steel columns, and the total steel amount of the CFT system is less by about 10% than that of steel system. Cost of the CFT main frames is lower by 5 to 7% than that of the steel frames; total building cost for the CFT system would be lower by 1% than that of the steel system if the cost of main frame structure is assumed to occupy 15% of the total building cost; as the number of stories increases, the cost merit of the CFT system becomes larger.

CFT structure also became a hot research topic during recently several decades in Japan. In 1961, Naka, Kato,et al., wrote the first technical paper on CFT in Japan.

In 1985, five general contractors and a steel manufacturer won the Japan's Ministry of Construction proposal competition for the construction of urban apartment houses in the 21st century. Since then, these industries and the Building Research Institute (BRI) of the Ministry of Construction started a five-year experimental research project called New Urban Housing Project (NUHP).

Another 5-year research project on composite and hybrid structures started in 1993 as the 5th phase of the U.S-Japan Cooperative Earthquake Research Program, and the program was organized into the following 4 groups: CFT column system; reinforced concrete + steel beam system; hybrid wall system; and research for innovation of new materials, elements and systems. The program of the Japanese side for CFT system consists of the following topics: experimental study; centrally-loaded stub columns, eccentrically loaded stub columns, beam-columns, and beam-to-column connections were tested to clarify synergistic interaction between steel tube and concrete and stress transfer mechanism, and to derive methods to evaluate stiffness, strength and ductility of CFT elements and systems.

The number of abstracts of technical papers on CFT column system presented at the annual meeting of Architectural Institute of Japan (AIJ) has been increasing every year, and more than 40 abstracts have been presented recent years. The have dealt with the following items: axial compressive stress-strain relations of concrete and steel tube; moment-curvature relation; ultimate strength, load-deformation relation and deformation capacity of a CFT beam-column; buckling strength of a CFT compression member; bond strength between concrete and steel tube; field tests of concrete casting; case study of CFT column systems.
Provisions for the design of CFT structures have been include in SRC Standards of AIJ and CFT recommendations were published by AIJ in 1997.

1.3 Problem Statement

Although the use of CFT columns with relatively thin-walled steel tubes column system has increased over the past several decades, all of the available information on connection details and design for composite construction is limited to the connection of CFT column-steel beam or CFT column-reinforce beam structure; no any research work information on CFT column-CFT beam system structure are available until now.
The employment of CFT beam can improve the stiffness of whole building, delay the local buckling of beam and improve fireproof performance of the whole building.
One of the obstacles that prevent CFT structure to be applied to beam is due to the need of vibrating compaction work of conventional concrete. Conventional concrete is able to be employed to make CFT column since the vibrating compaction work along vertical direction is easy to be practiced, whereas, it is difficult to compact the conventional concrete along horizontal direction in the beam. Therefore, only CFT column system is popularly used in the present practical applications.
In order to make it possible to apply CFT structure to beam, thus construct CFT column-CFT beam frame structure, self-compacting concrete (SCC) was proposed in this research. SCC has the advantage of being able to be compacted into every corner of a formwork purely by means of its own weight without the need of vibrating compaction. This character of SCC makes it possible to apply CFT structure to beam.

1.4 Research Objectives

A good structural system must be evaluated in four aspects; the cost performance, the fabrication, the quality assurance, and the structural performance.

According to the former experiences in the building construction industry, one weak

point of the CFT system is the compactness of concrete around the beam to column connection, especially in the case of inner and through-type diaphragms, in which the gap between concrete and steel may be produced by the bleeding of the concrete underneath the diaphragm. In this research, SCC is proposed to be cast into the CFT column-CFT beam frame structure. The objective of investigating compactness quality of SCC was carried out through experimental work.

One of the most important issues in using the new proposed CFT column-CFT beam frame structure in construction is identifying a suitable joint detail for connecting CFT beams to CFT columns. A suitable joint detail should be constructed conveniently by the fabricators as well as lead to economy of composite construction. The former viewpoints tend to be neglected by the people in academia. Cooperation with designers and fabricators will be essential for this research. Different beam-column joint details were designed and compared in this research.

Another main objective of this research is seismic behavior investigation of the new proposed CFT column-CFT beam frame structure in order to confirm whether this structure is suitable to be applied to seismic region. For this purpose, several subassemblies were made and tested and the inelastic cyclic behavior of the CFT column-CFT beam frame joints were investigated and understood.

Furthermore, an objective is focus on the construction method for this new CFT column-CFT beam frame structure in order to make it possible to efficiently pour concrete into the new frame structure in the building site. The new construction method is developed based on the existing bottom up pumping method for CFT column system. In order to verify the feasibility of this proposed construction method, visual model of fresh concrete experiment was employed to simulate the real pouring situation.

Once a new kind of structure is proposed, the most important key point should be considered is whether this new proposed structure has sufficient properties basing on higher cost performance compared with the existed structure.

The final objective in this research is to investigate the cost performance of the new CFT column-CFT beam frame structure. The cost of the new CFT column-CFT beam frame structure was compared with the cost of conventional steel structure based on building frame designs using both kinds of structures.

1.4 Dissertation Scope and Layout

The overall philosophy taken in this research is to first investigate the compactness quality of SCC, design and choose suitable connection detail, understand the seismic behaviour of the chosen connection detail, once the advantage of the new CFT structure is confirmed, the following step is to develop a feasible construction method for the new structure to make it convenient and efficient for the new CFT structure to be constructed in the real building site. Finally also investigate the cost performance of the proposed CFT column-CFT beam frame structure to make sure that this new structure also has cost advantage.

Chapter 2 provides the connection details of each specimen, summary of seismic behavior investigation experimental program and results.

Base on the existing bottom up pumping method for CFT column-steel beam system and the unique character of the new proposed CFT column-CFT beam system, a special construction method is developed in order to make it possible to efficiently cast concrete into the new frame structure in the building site. Chapter 3 describes this special construction method in detail. The content include decision of number of input ports, the possible story number in one SCC pouring period and the possibility of decrease in construction cost and project time by employing branch pipe.

After the special construction method for new CFT column-CFT beam frame structure was proposed, further research work was conducted for the purpose of observing the flow situation of concrete. Chapter 4 presents the experimental work of investigation of construction method using visual model of fresh concrete. The simulation mechanism of visual model and experimental results is described in this chapter.

Chapter 5 presents the trial design of theme structures and the cost comparison between proposed CFT column-CFT beam frame structure and conventional steel structure. Theme structures treated in this research are 9, 18 and 40 stories unbraced building frames made of both CFT column-CFT beam frame structure and conventional hollow steel tube-H beam steel structure. Firstly, the design and analysis details were described; subsequently the cost performance of both structures was presented. In order to investigate whether the connection is able to meet the level of force and ductility requirement, four 56% scale specimens, three CFT column-CFT beam connections and one hollow steel column-I beam connection, which based on a real prototype building

were made and tested.

Conclusions and main findings of the research are summarized in Chapter 6. Suggestions for further areas of research are provided in Chapter 6 as well.

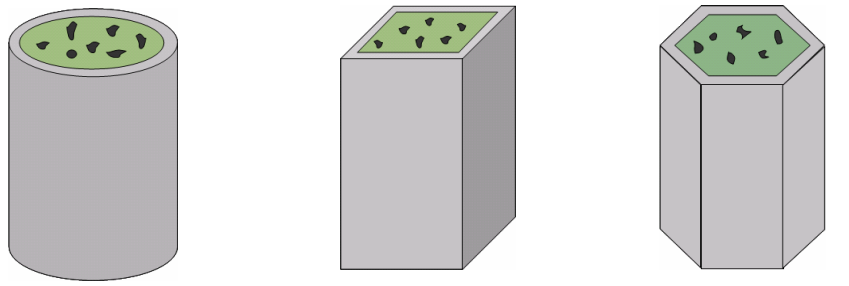

Circular CFT | Rectangle CFT (Square CFT) | Polygon CFT

Fig1.1 CFT Structure

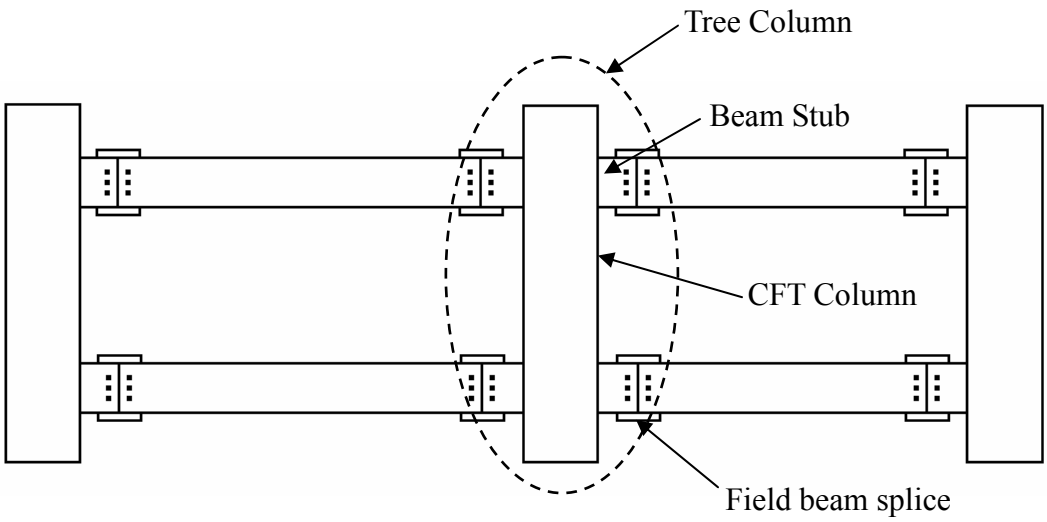

Fig1.2 Tree Column Construction Concept

CHAPTER 2

EXPERIMENTAL RESEARCH ON SEISMIC BEHAVIOR OF NEW CFT COLUMN-CFT BEAM FRAME STRUCTURE

2.1 Introduction

Self-compacting concrete (SCC) is employed to the new CFT column-CFT beam frame structure in this research.

SCC can be compacted into every corner of a formwork purely by means of its own weight without need of vibrating compaction. However, the compacting quality of SCC in the new CFT column-CFT beam frame structure is still need to be investigated since no information on this research is available until now.

In this part of research program, the compacting quality of SCC was understood by experimental work. The investigation result is presented in this chapter.

Furthermore, this chapter describes joint details of the new CFT column-CFT beam frame structure. The experimental results of four specimens, three square section CFT column-CFT beam connection specimens and one square section hollow column-I beam connection specimens, are also presented in this chapter.

Notation

f_y	yield stress	t	V-funnel of SCC
f_u	ultimate strength	Φ	slump flow of SCC
f'_c	concrete compressive strength		
P_y	nominal yield load of beam		
δ_y	yield beam tip deflection		
M_p	nominal plastic moment capacity of beam		

2.2 Joint Representation

Fig2.1 (a) shows the deflected shape of a structural frame subjected to lateral loading. The moment distribution in such a frame is characterized by having inflection points near the midpoints of the beams and columns. Due to lateral loads, the columns in the frame are subjected to shear forces and lateral deformations. The deformed shape of an interior joint can be idealized as shown in Fig 2.1 (b). The geometry of the test specimen was selected to represent an interior joint in a building subjected to lateral

load. Each of the tested specimens had a cruciform shape and consisted of a CFT column and two parts of CFT beams were linked to the column. The specimens were approximately 56% scale compared to the member sizes which was taken form a prototype building. The ends of the beam and column of the test specimen corresponded to the inflection points, which were assumed to be at midpoints of the corresponding members in the prototype building.

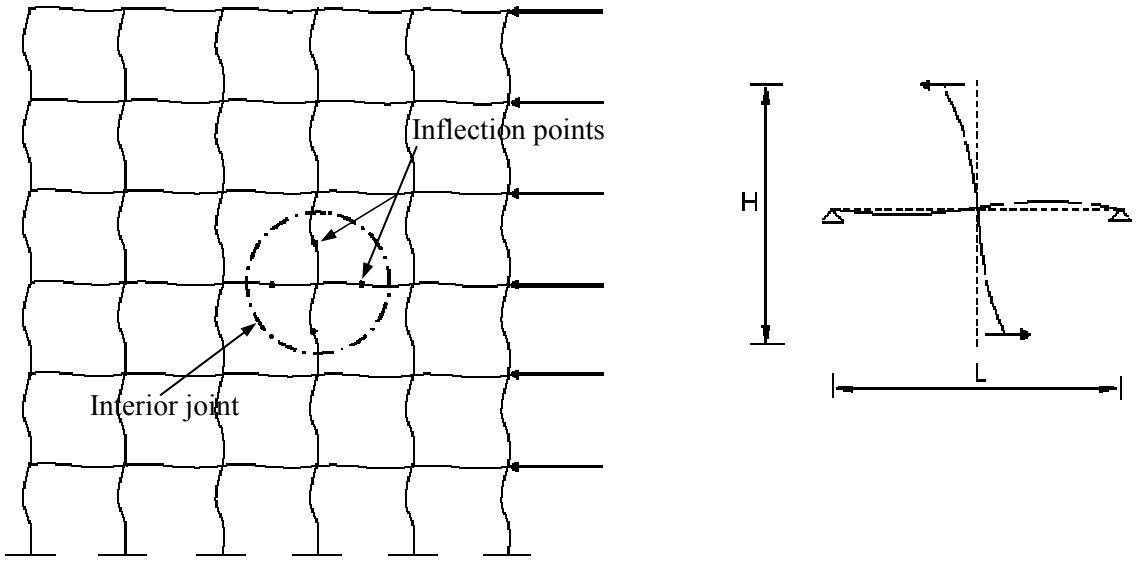

(a) Frame Subjected to Lateral Loads (b) Idealized Interior Joint

Fig2.1 Modeling of Beam-column Subassembly Interior

2.3 Joint Detail Design

There are some typical joints which were used for CFT column-steel beam frame system. Fig2.2 shows the joint details.

A suitable joint detail for the new CFT column-CFT beam frame structure should meet the strength, deflection and ductility requirement. One the other hand, the joint detail should be constructed conveniently by the fabricators as well as lead to economy of composite construction. Form these viewpoints, two different CFT column-CFT beam joint details, outer-diaphragm joint detail and PC bar linked joint detail were designed and compared in this research.

The outer-diaphragm joint detail is shown as Fig2.3 (a); the two parts of left and right beam were welded to the column by four pieces of steel plates. PC bar linked joint detail is shown as Fig2.3 (b); the two parts of left and right beam were linked to the column by 10 PC bars.

Ring Stiffener

Long Stiffener

Inner Diaphragm

Horizontal Triangle Stiffener

Tension Joint with High-strength Bolt

Vertical Stiffener

Fig2.2 Typical Beam-column Joints

2.4 Experimental Text Program

2.4.1 Test Specimen and Material Properties

Totally four specimens were made and tested in this part of research program. One hollow steel column-I beam specimen and three CFT column-CFT beam specimens. All the specimen joint details are shown in Fig2.3. Outer-diaphragm joint detail was employed to pure steel specimen. Two PC bar linked joint detail specimens were made. Difference between these two PC bar linked joint detail specimens is that partial penetration weld and full penetration weld were applied to them respectively.

The four specimens were called CDF, CPP, CPP_1 and SDP_1. The notation used for each specimen gives structure type (‘C’ for CFT structure, ‘S’ for steel structure), joint method (‘D’ for diaphragm, ‘P’ for PC bar) and weld method (‘F’ for fillet weld, shown in Fig.2.3 (a); ‘P’ for partial penetration weld, shown in Fig.2.3 (b); ‘P_1’ for full penetration weld, shown in Fig.2.3 (c)).

All beams of CFT joint specimens had same section dimensions and same nominal moment capacity. Nominal moment capacity of I beam approaches CFT beam. Cross Section Dimensions of each specimen is shown in Fig.2.4.

Table 2.1 shows material properties of specimens. Table2.2 shows mix-proportioning of

SCC.

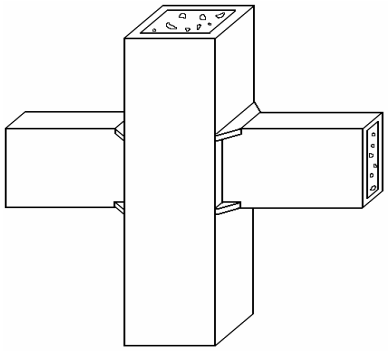

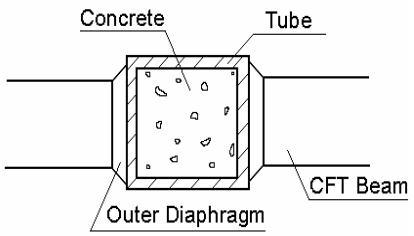

(a) CDF

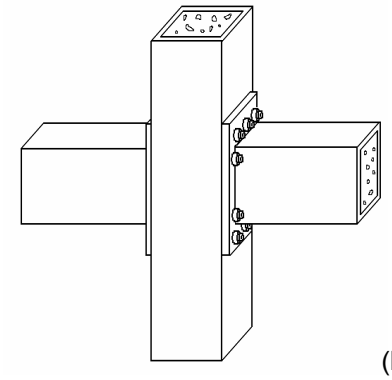

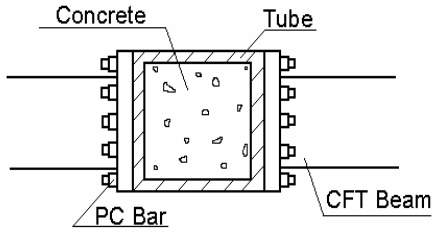

(b) CPP, CPP_1

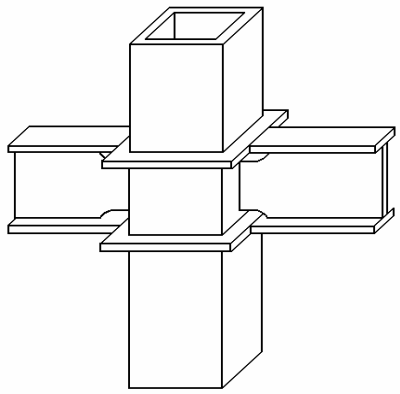

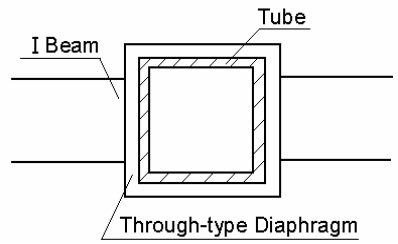

(c) SDP_1

Fig2.3 Specimen Joint Details

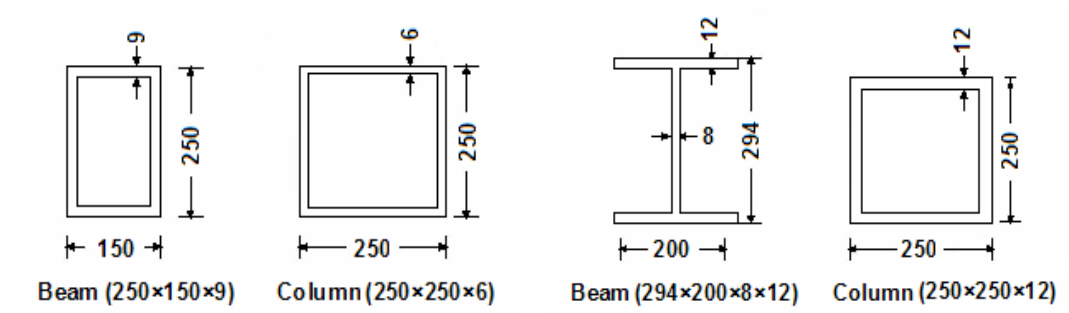

(a) CDF, CPP, CPP_1 (b) SDP_1

Fig2.4 Cross section dimensions of beams and columns (mm)

Concrete was cast from the top of columns in the experimental work. It may flow along the directions similar to the arrows shown in Fig.2.5 (a), (b), and (c). Air entrapment may easily occur at each corner of the connected regions. Four 4mm holes were drilled on each beam as Fig.2.5 (d) shows to drain off the inner air of the beam. Diameters of these holes were so small compared with dimensions of beam that their existence did not affect load capacity of beams. After concrete was poured into the specimen, it overflowed from the holes which indicated a good compacting result. Fig2.6 shows the situation after compacting of SCC.

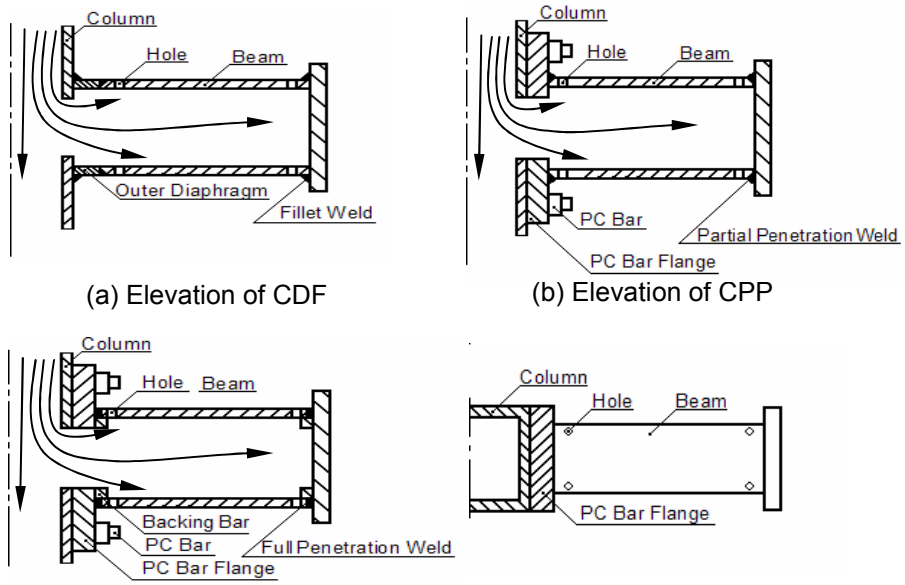

(a) Elevation of CDF (b) Elevation of CPP

(c) Elevation of CPP_1 (d)

Fig2.5 Beam Details of Specimens CDF, CPP, and CPP_1

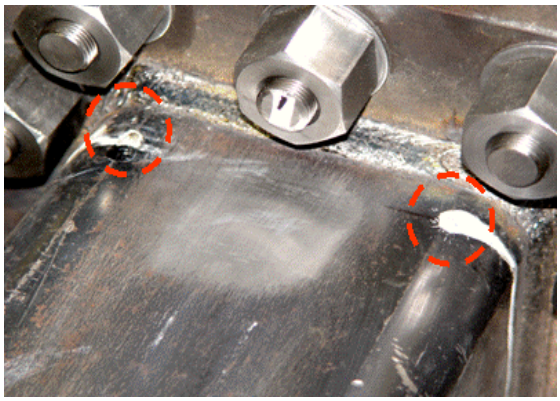

Joint Position of Left Beam

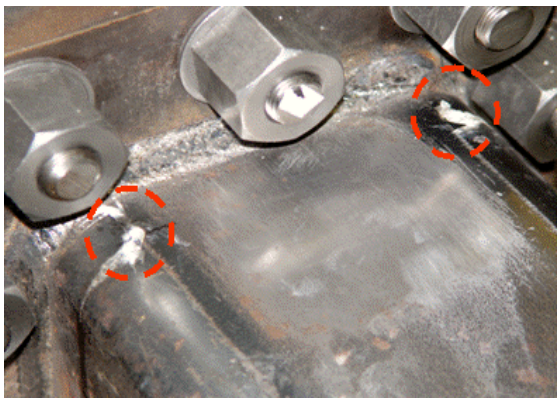

Joint Position of Right Beam

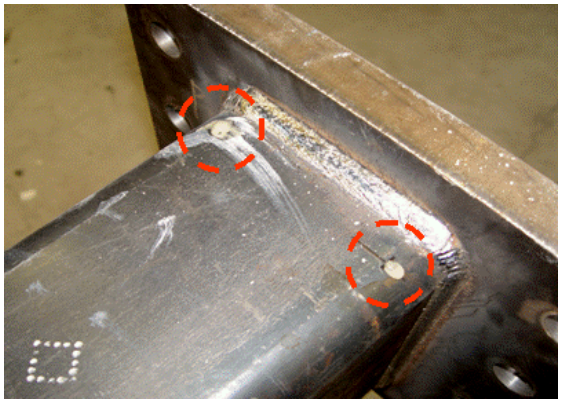

End of Left Beam

Right of Left Beam

Fig 2.6 Confirmation of Compacting Quality of SCC

Table2.1 Material Properties of Connection Specimens

	Specimen	CDF	CPP	CPP_1	SDP_1
Beam	f_y (MPa)	245	245	245	245
	f_u(MPa)	400	400	400	400
	M_p(KN m)	181.5	181.5	181.5	185
Column	f_y (MPa)	325	325	325	325
	f_u (MPa)	490	490	490	490
Concrete	f'_c(MPa)	76.2	79.1	80.2	-----
	t (S)	13.9	13.0	14.2	-----
	Φ (mm)	650	680	730	-----

Table2.2 Mix-proportioning of SCC (kg/m^3)

W/C	C	W	Fly Ash	S	G	Ad
34.5	492	170	170	851	772	9.6

2.4.2 Test Setup and Instrumentation

Fig2.7 shows a photograph of the test setup with a typical specimen. The column was subjected to a constant axial load representing the reaction received from floors. Equal and opposite vertical loads were applied at the beam ends to simulate the deformed shape of an interior joint in a building subjected to lateral loads. The column ends were restrained from horizontal movement but were allowed to rotate in the plane of loading. Two beam ends were restrained with jacks and were allowed to rotate in the plane of loading.

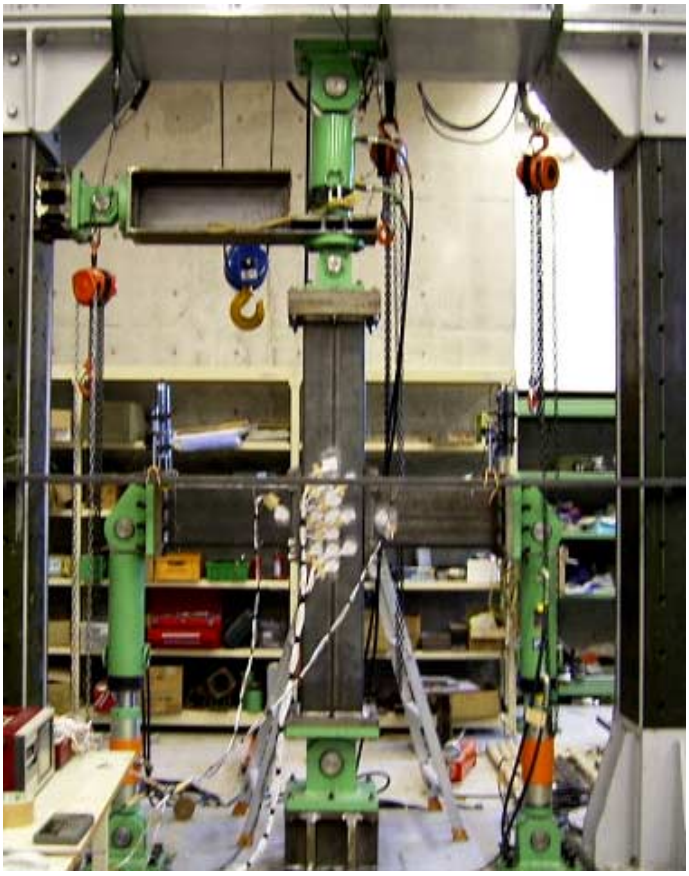

Fig2.7 Photograph of Column Test Setup

1000 KN axial loads were applied to the columns first. This value was remained constant during the whole period of test. Equal and opposite vertical loads were then cyclically applied to the end of the beam. A typical cyclic load history of beam is shown in Fig.2.8. The first two cycles were conducted under load control, the values of loads were 30%, 60% of P_y. The following cycles were conducted under deflection control during inelastic stage.

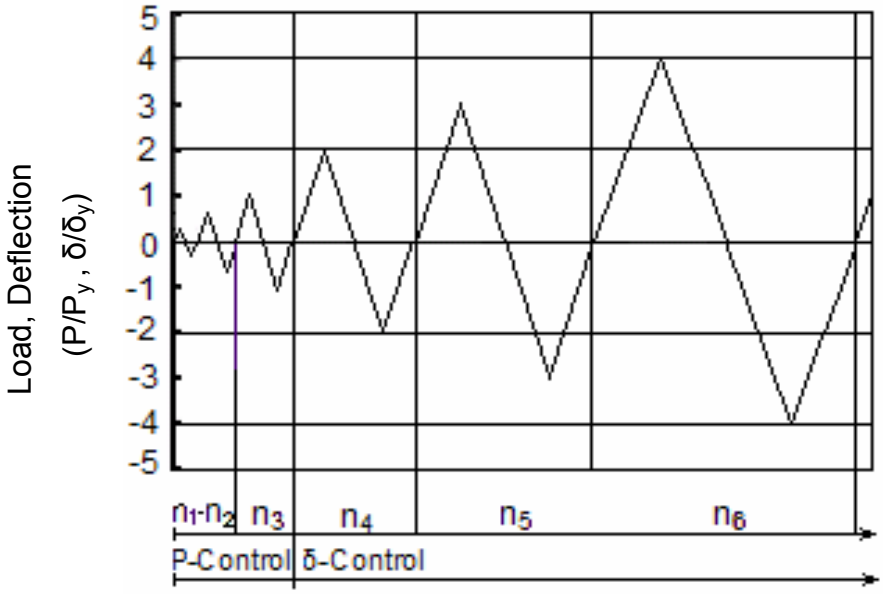

Fig2.8 Cyclic Load History

The specimens were instrument to measure applied loads, displacements and strains at different locations. Displacement transducers were employed at the end of each beam to obtain the displacement. Applied loads at each stage were measured by load cells which connected with jacks. Triaxial strain gauges and monoaxial strain gauges were respectively attached to the joint panel, columns and beams surface which near to the joint panel, to study the state of stress in those regions. The distribution of instrumentation was shown as Fig2.9.

2.5 Test Results and Discussion

Load-drift angle responses were used to compare the performance of each connection. The drift angle of the specimen was calculated as the ratio of the total relative vertical

displacement between the two ends of the beam to the distance between the two ends.

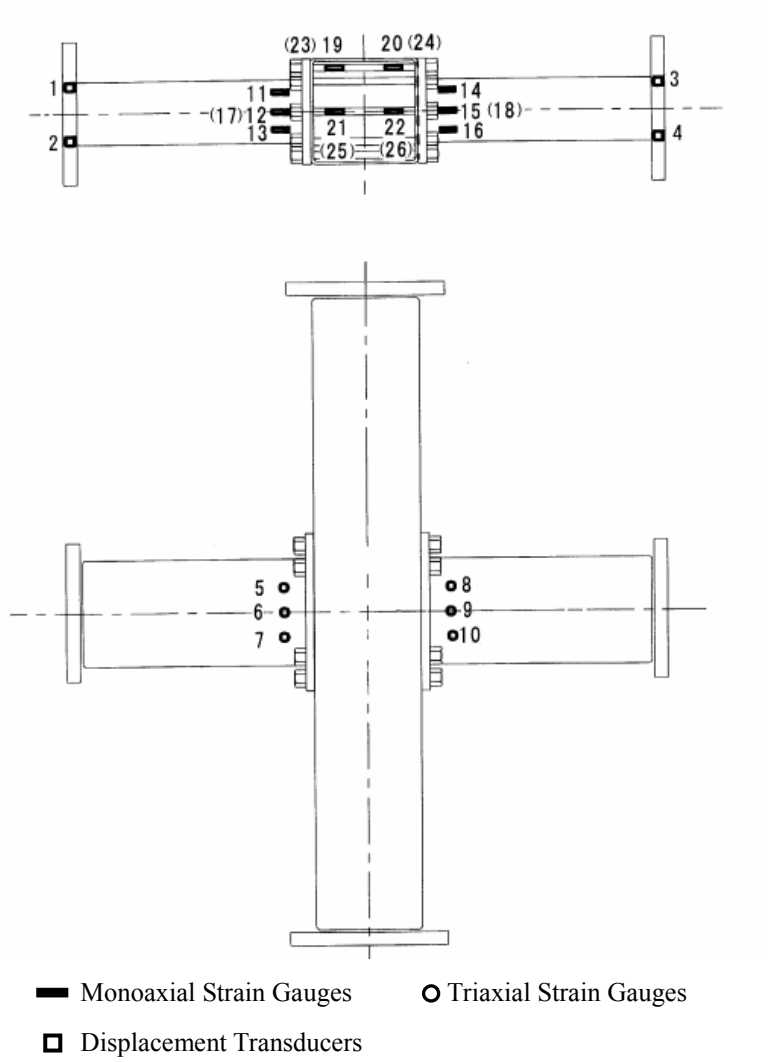

Fig2.9 Distribution of Instrumentation

2.5.1 Specimen behaviour

Fig2.10 shows load-drift angle response of specimen CDF. The maximum Load obtained during the test was 247KN at 1.7% drift angle. The specimen was able to develop 91.8% of plastic moment capacity of beam. Failure due to precocious fracture of fillet weld attached beam to column, which is shown in Fig2.11.

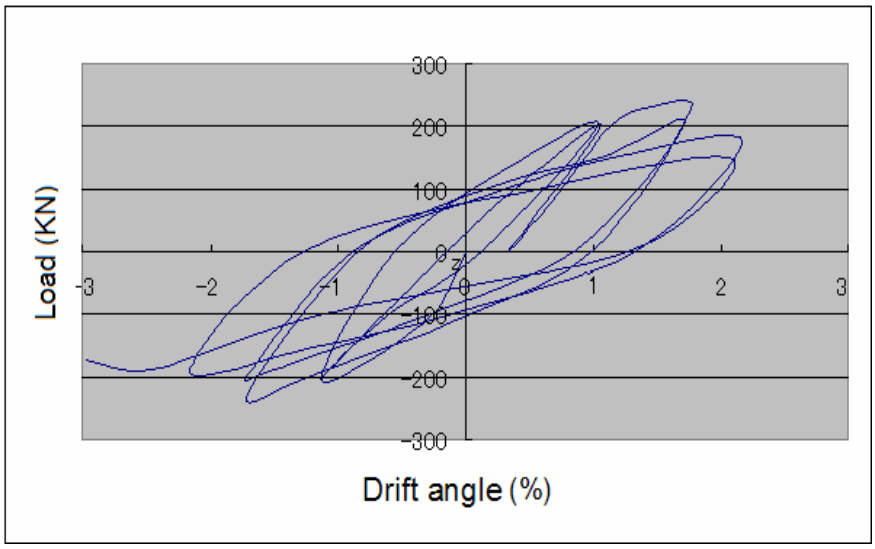

Fig2.10 Load-drift Angle Response of Specimen CDF

Fig2.11 Weld Fracture in Specimen CDF

Fig.2.12, Fig.2.13 shows load-drift angle response for specimens CPP and CPP_1. Different maximum Loads obtained form two specimens due to different weld method employed to them, 278KN at 5.5 % drift angle for CPP, 211.5KN at 7.8% drift angle for CPP_1. They were able to develop 120%, 132% of plastic moment capacity of beam respectively. The maximum beam tip deflection for CPP was $3\delta_y$; while for CPP_1 was $4\delta_y$. Both of them failed due to weld fracture shown in Fig2.14 and Fig2.15. Insufficient thickness of PC bar flange led to a little larger deformation of PC bar flange. Fig2.16

shows the deformation situation of PC bar flange.

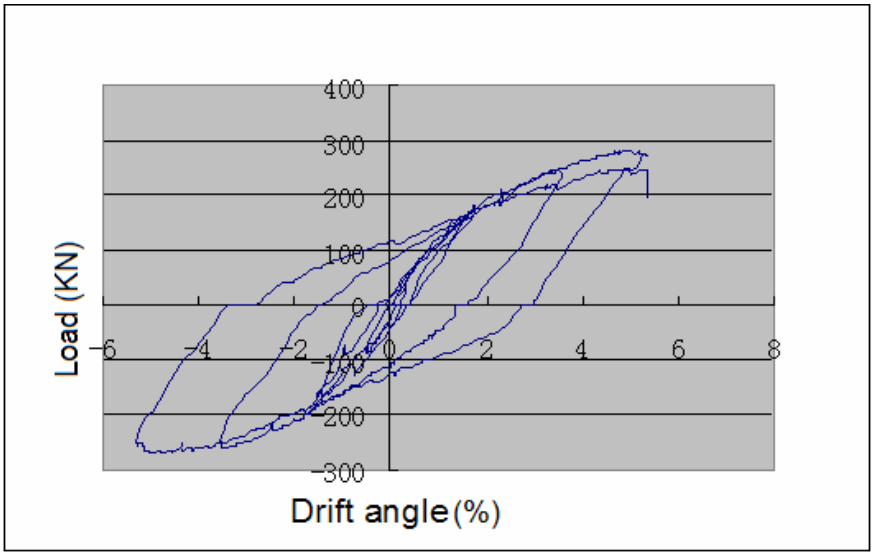

Fig2.12 Load-drift Angle Response of Specimen CPP

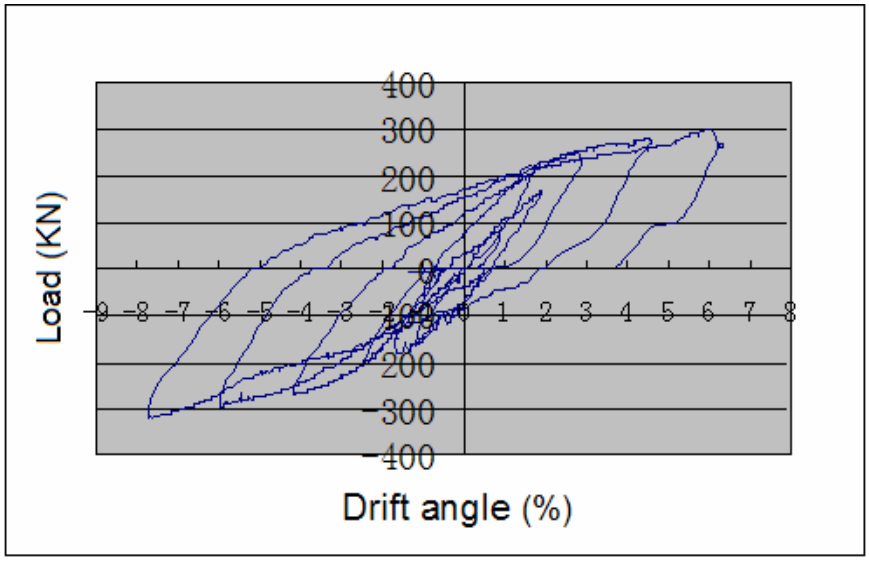

Fig2.13 Load-drift Angle Response of Specimen CPP_1

Fig2.14 Weld Fracture in Specimen CPP

Fig2.15 Weld Fracture in Specimen CPP_1

Fig2.16 Deformation of PC bar Flange

Load-drift angle response of specimen SDP_1 is shown in Fig2.17. No weld fracture occurred since through-type diaphragm and full penetration weld were employed in the specimen. The test had to be terminated due to overstepping the load capacity of jack. Maximum Load was not able to be obtained.

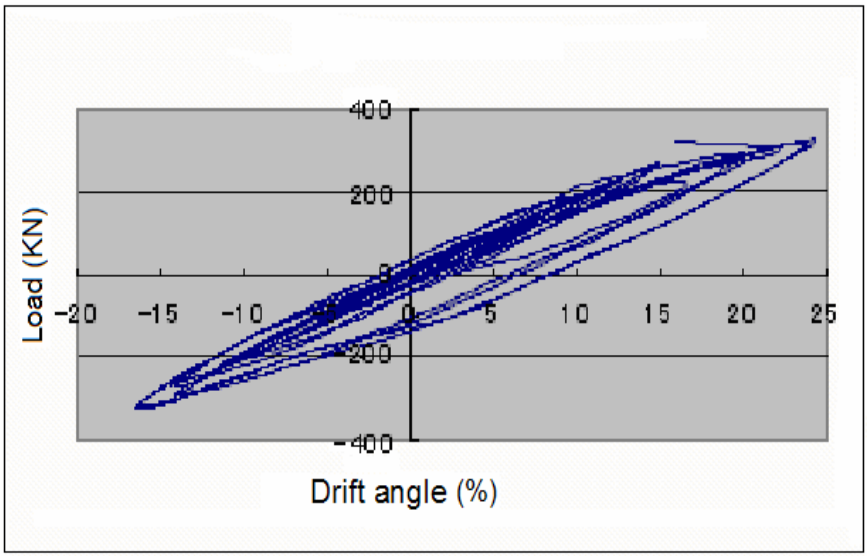

Fig2.17 Load-drift Angle Response of Specimen SDP_1

2.5.2 Discussion

Failures of all CFT connection specimens were due to fracture of the weld that attached the beam flange to tube or PC bar flange. Specimen CDF was not able to develop plastic capacity of beam due to precocious weld fracture. Specimen CPP and CPP_1 were not able to develop full plastic capacities of the beam due to the brittle weld fracture. Specimen SDP_1 was inferred able to develop further plastic capacity since no failure occurred until end of test. However, specimen CPP_1 exhibited higher maximum load capacity and ductile behavior compared with Specimen CPP due to different weld method. The hysteresis loops of CFT connection specimens were plumper than that of steel connection specimen, which indicated a higher energy dissipation capability of CFT connections.

2.6 Conclusions

According to the research work present above, several conclusions are made and list below.

1)The experiment result shows that self-compacting concrete (SCC) can be successfully compacted into beam tube, which indicates that CFT column-CFT beam frame can be made using SCC.

2) The substantial deformation capacity expected was obtainable in two PC bar jointed CFT column-CFT beam connection specimens. Insufficient thickness of PC bar flange led to a little larger deformation of PC bar flange. Increase of the thickness is inferred able to strengthen the connection.

CHAPTER 3

CONSTRUCTION METHOD FOR NEW CFT COLUMN-CFT BEAM FRAME STRUCTURE

3.1 Introduction

In the experimental research work, it had been confirmed that self-compacting concrete (SCC) is able to be compacted into the CFT column-CFT beam subassembly successfully. However, from viewpoint of practical application for a whole building, the most important issues in using the new CFT column-CFT beam frame structure system is developing an efficient construction method which can lead to decrease of manpower, construction cost and project time.

In this part of research work, according to the structural characteristics of this new frame structure, a new bottom up pumping method, different from the existing method used for CFT column system, was developed.

Chapter3 presents the innovation of the developed the bottom up pumping method. An example of application this new developed construction method to the 9-story building frame which were designed in the former building frame design research program, is also described in chapter3 in order to show the advantage of this new construction method.

Amount of mortar of flesh concrete will attach on the inner surface of steel tube during the whole construction process. In order to investigate that whether the consumed amount of mortar is able to lead to segregation when concrete drop form top of the steel tube to the bottom, experimental work of concrete flow test was conducted in this part of research program.

3.2 Idea of New Developed Construction Method

3.2.1 Construction Method for CFT Column System

Four kinds of construction method already exist for CFT column-steel beam frame structure. These construction methods are described in detail in Recommendations for Design and Construction of Concrete Filled Steel Tubular Structures (ANUHT, 2002).

High-dropping construction method

After the construction of steel tube of CFT column, steel beam and slab, concrete is dropped form top to the bottom of steel tube by some tools. During the whole

construction period, the tools are elevated step by step; amount of concrete is poured into the steel tube after each elevation of the tool until the whole steel tube is filled with concrete. This construction method is suitable for the case that the drop-height is relatively lower.

Tremie tube construction method

In order to avoid the segregation of concrete occurred, tremie tube is linked with circular pipe, a poker vibrator vibrating needle is attached to the top of tremie tube; concrete falls form top of the tube to the bottom through the pipe and tremie tube. Vibrating compaction work is done simultaneously during the concrete casting period. Fig3.1 (a) shows tremie tube construction method schematically.

Sunny hose construction method

Concrete is poured into the hopper which above the hose, the space inside the hose is relatively commodious, thus concrete is able to smoothly fall to the bottom along the inner surface of tube. This kind of construction method can decrease the air entrapment occurring in concrete. Fig3.1 (b) shows sunny hose construction method schematically.

Bottom up pumping method

After the construction of steel tube of CFT column, steel beam and slab, concrete is poured into the steel tube from bottom to top through an input port, which located on the bottom of the steel tube by pump car. Consider about the existence of inner diaphragm in some joint detail, in order to insure compaction quality beneath the inner diaphragm, this kind of construction method is normally used for high flow ability concrete. Fig3.1 (c) shows bottom up pumping method schematically. Fig 3.2 shows the input port detail.

3.2.2 Innovation of New Construction Method

Among the four construction methods described above, high-dropping construction method, and sunny hose construction method is normally used for ring stiffener and outer diaphragm joint detail since there has no any barrier inside the steel tube and tool is easy to be insert inside it. However, difficulty in properly compacting the concrete may create a weak point in the system in the case of inner diaphragm and through-type diaphragm where bleeding of the concrete beneath the diaphragm may produce a gap between the concrete and steel. Therefore, for inner diaphragm and through-type diaphragm, bottom up pumping method is popularly used instead of the former

construction methods.

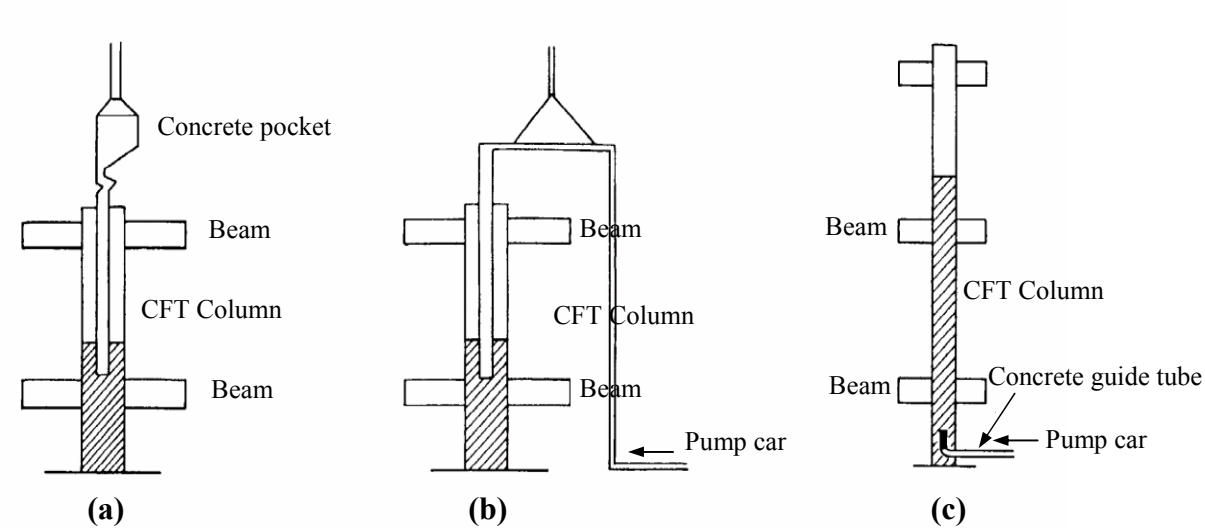

Fig3.1 Construction Method for CFT Column-steel Beam Frame Structure

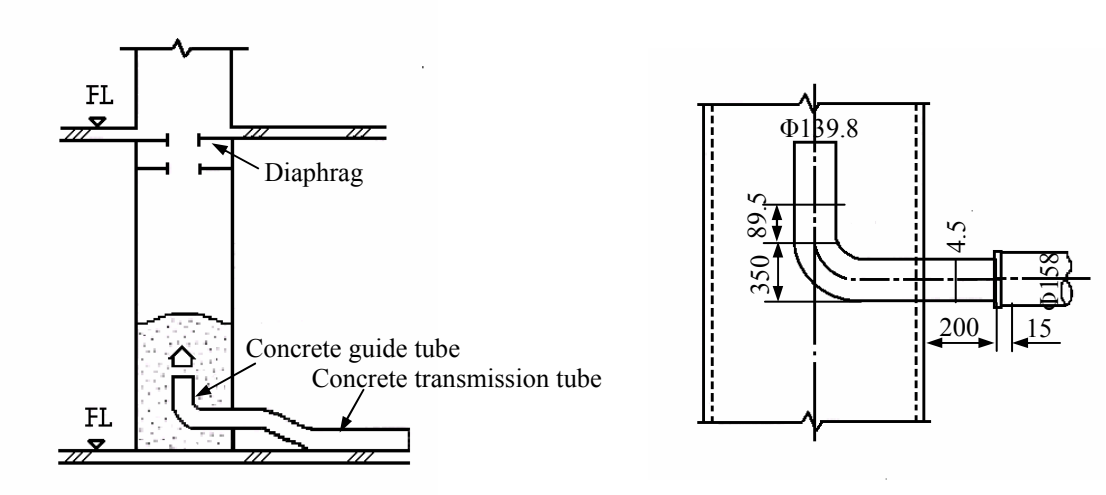

Fig3.2 Detail of Input Port

According to the result of the experimental work on seismic behavior of the new CFT column-CFT beam frame structure, which was presented in chapter2, it was confirmed that the PC bar linked joint detail is a kinds of more suitable joint detail for the new CFT structure. The PC bar linked joint detail employs 10 PC bars and these PC bar cross through the joint panel. Therefore, the construction method for the new CFT column-CFT beam frame structure was developed basing on the existed bottom up pumping method due to the character of the PC bar linked joint detail.

In the application of bottom up pumping method to CFT column-steel beam frame system, each steel tube of the column has to be made an input port in order to pour concrete to the whole building frame. Whereas, CFT column-CFT beam frame system has the advantage that all the beams and frames have connectedness, concrete can flow form one column to another column through the beam which links the two columns. The character of this new CFT column-CFT beam frame structure makes it possible to construct concrete to the whole building frame only through several input ports which are made on several columns.

In the ideal of new construction method for the new CFT column-CFT beam frame structure systems, branch pipe is also be considered to be employed. All the input ports are able to be linked together using the branch pipe to one pump car to construct the concrete, which can lead to the decrease of construction time and cost.

3.2.3 An Example of Application of New Developed Construction Method

Take one framing floor plan which is shown in Fig3.3 as an example to explain the application of the new developed bottom up pumping method concretely.

3.2.3.1 Decision of Member of Input Port

As former explained, only certain of input ports are needed to be made on certain of columns due to the character of CFT column-CFT beam frame structure. Therefore, the key point in application of the new developed bottom up pumping method is the decision of member of input ports.

According to the Recommendation for Self-compacting Concrete (JSCE, 1999), the maximum lateral flow distance for SCC is around 15 meter. Assuming that SCC also can flow such distance and basing on the dimensions of the frame which is taken into example, only 8 input ports are needed to be made. The locations of these input ports are shown in Fig3.3.

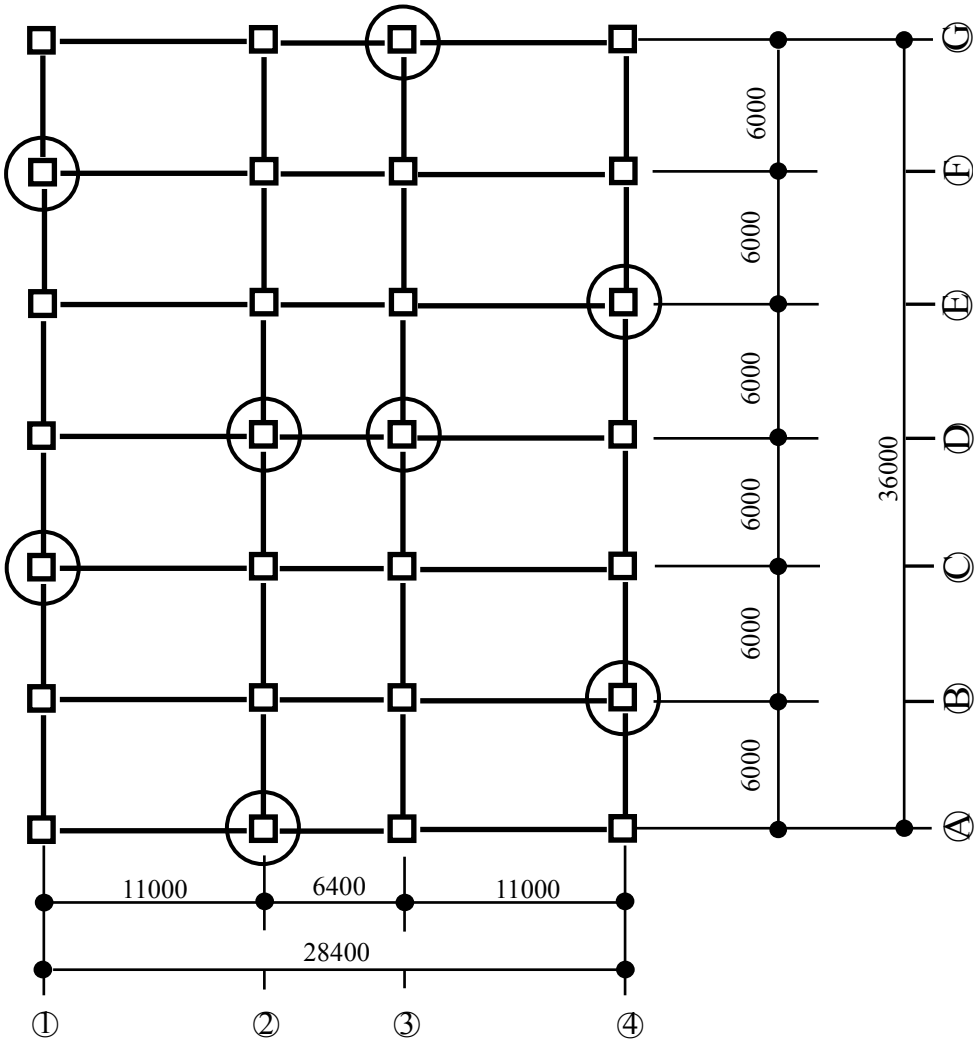

Fig3.3 Location of Input Ports on Framing Floor Plan

3.2.3.2 Concrete Casting Speed and Casting Height

The concrete should be cast within 90 minutes in one casting period in order to insure good flow ability of concrete. According to the building frame design, the average volume of concrete need for columns and beams of two stories is 90m^3. Therefore, the casting speed should be 1m^3/min. When this value is distributed to 8 columns with input ports, the pouring speed is within 1m/min which in accord with Recommendations for Design and Construction of Concrete Filled Steel Tubular Structures (ANUHT, 2002).

The analysis result indicate that it is possible to pour two stories in one pouring period using this new developed bottom up pumping method, furthermore, branch pipe is also employed to decrease the number of pump car, thus lead to decrease of construction cost

and project time. The image of this construction method is show schematically in Fig3.4.

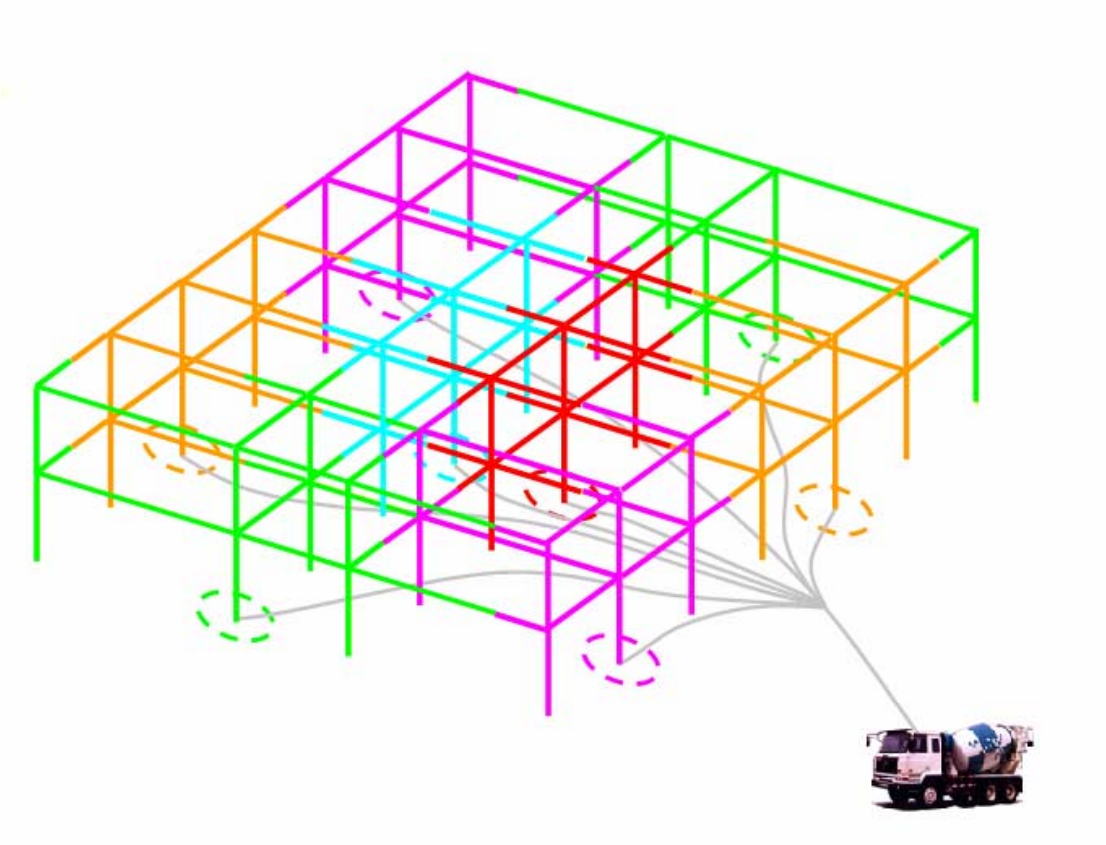

Fig3.4 Image of New Developed Bottom up Pumping Method in Building Site

3.3Experiment on Investigation of Thickness of Mortar Which Adheres to Steel Plate Surface

Mortar may attach on the inner surface of the steel tube during concrete flows through the tube. If the amount of mortar which attaches on the inner surface is large, coarse aggregate will concentrate to the front of concrete flow; this may lead to segregation of concrete when concrete drops from top to the bottom of steel tube since coarse aggregate may fall down firstly to the bottom of the steel tube. The image of this situation is shown in Fig3.5. The occurrence of segregation, thus, affects durability of the whole structure.

In order to further investigate the amount of mortar which attach on the inner surface of

steel tube, an experimental work which simulates the flow of concrete inside the steel tube was done using some available tools in the laboratory.

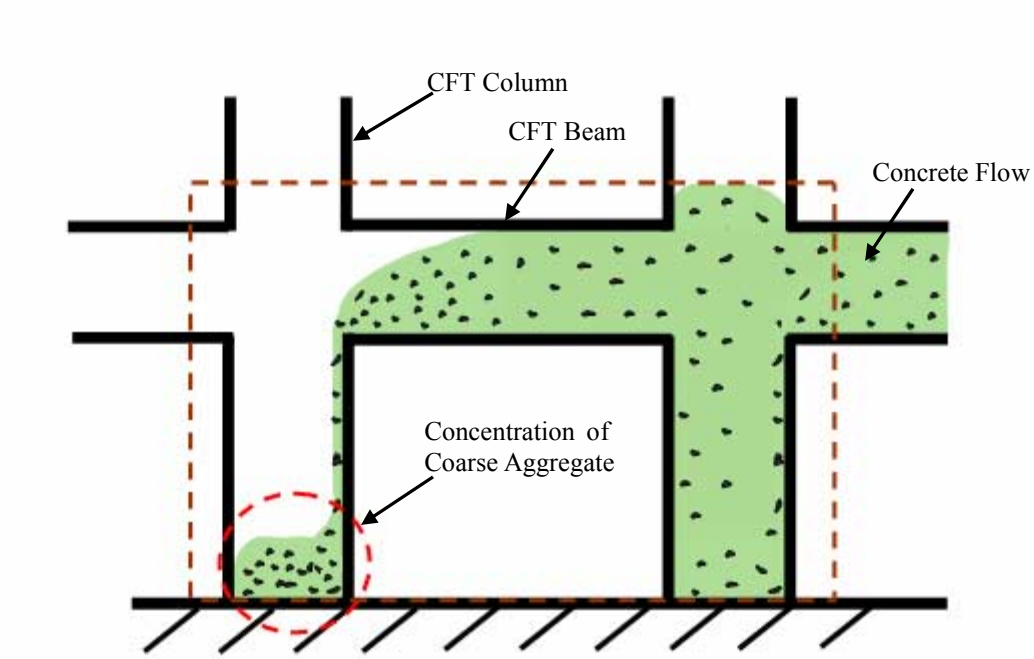

Fig3.5 Image of Segregation

3.3.1 Test Setup and Material Property

A typical test setup for concrete flow simulation test is shown as Fig3.6. A steel trough was fabricated with a slope angle of and a v-funnel was disposed at the end of the steel trough, which served as a pocket, thus concrete fall to the steel trough through it. Fig3.7 (a) and (b) shows the dimensions of steel trough and v-funnel which used in the test respectively. Capacity of v-funnel is 11.3 L; inner surface area of v-funnel is 0.395m^2.

In the concrete flow simulation test, totally three kinds of mix-proportioning of SCC were tested. Water cement ratio and dosage of superplasticizer are different among these three mix-proportioning which aims to obtain different viscosity of SCC, thus investigate the effect of viscosity to the amount of mortar which attached on the inner surface of the steel trough. The three mix-proportioning of SCC are shown in Table3.1, Table3.2 and Table 3.3 respectively. Table 3.4 shows the slump flow and v-funnel time of these three mix-proportioning which reveals that these three mix-proportioning have closed slump flow value while different v-funnel time.

Fig3.6 Test Setup of Concrete Flow Test

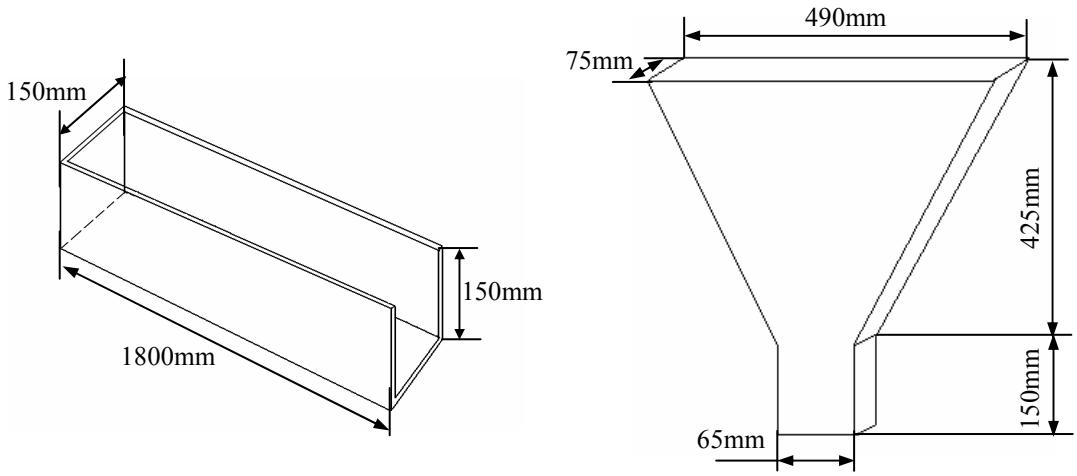

(a) Steel Trough (b) V-funnel

Fig 3.7 Dimensions of Tools

Table3.1 Mix-proportioning 1 (Kg/m^3)

W/C	Air	W	C	S	G	SP
26.1	1.3	171.9	658.5	826.0	823.2	8.5

Table3.2 Mix-proportioning 2 (Kg/m^3)

W/C	Air	W	C	S	G	SP
25.3	1.0	169.7	669.5	828.0	825.7	9.22

Table3.3 Mix-proportioning 3 (Kg/m^3)

W/C	Air	W	C	S	G	SP
24.7	0.9	167.4	678.0	829.0	826.5	9.78

Table3.4 Slump Flow and V-funnel of Three Mix-proportioning

	Mix-proportioning 1	Mix-proportioning 2	Mix-proportioning 3
Slump Flow (mm)	622 ×640	650 ×645	640 ×596
V-funnel time (sec.)	9	12	30

3.3.2 Test Program

Considering that the original designed mix-proportioning of SCC may changed after it passes through a clean V-funnel and fall down to the steel trough due to some mortar may attached on the inner surface of funnel, the following experiment steps were conducted.

1. Recording the weight of clean V-funnel
2. Pouring concrete into v-funnel
3. Concrete passes through v-funnel (v-funnel time test)
4. Recording the weight of V-funnel with mortar adhered on the inner surface of it.
5. Pouring concrete into v-funnel again and recording the weight of funnel with

concrete.

6. Concrete passes through v-funnel, and then flows through steel trough. Recording again the weight of V-funnel with mortar adhered on the inner surface of it.
7. Taking one bucket of concrete which flow out form the steel trough every 5 second; totally 12 bucket of concrete were taken; recording each weight of concrete in each bucket.
8. Measuring the height and length of area attached with mortar of inner surface of steel trough.

As described above, concrete passes through V-funnel two times. After step 5, concrete falls down through V-funnel for the second time, and few mortar attached on the inner surface of v-funnel since the inner surface already was attached by mortar in step 3. This was verified by the test result that two values of V-funnel weight which were taken in step 4 and step 6 were almost same. Therefore, it can be assumed that the original designed mix-proportioning of SCC does not change after concrete passed through v-funnel and flowed inside the steel trough.

Basing on this assumption, the thickness of mortar which attached on the inner surface of steel trough was analyzed and calculated.

Fig3.8 shows the situation of V-funnel attached with mortar. Fig 3.9 shows the situation that after concrete flow through the steel trough.

3.3.3 Test Result and Discussion

After getting the weight of each bucket of concrete as explained in step 7 of the former section, mortar of concrete was washed off and pure coarse aggregate weights of the 12 bucket were recorded. According to the weights of concrete and coarse aggregate which were obtained, the weight ratio of coarse aggregate and concrete and volume ratio of mortar and concrete can be calculated. Fig 3.10 (a) and (b) shows the weight ratio of coarse aggregate and concrete and volume ratio of mortar and concrete of mix-proportioning 1 respectively. Fig 3.11 (a) and (b) shows the corresponding information of mix-proportioning 2. From Fig 3.10 and Fig 3.11, it reveals that with the increase of the amount of concrete which flowed out through the steel trough, the weight ratio of coarse aggregate decreased while the volume ratio of mortar increased, finally both of them arrived to the original designed value respectively. This result indicates that due to the attachment of mortar to the inner surface of steel trough, coarse aggregate concentrated to the front of concrete flow when concrete flowed through the clean inner surface of steel trough. After the inner surface of steel trough was attached

by the mortar, the mortar of later coming concrete tended to not attach on the inner surface anymore.

Weight ratio of coarse aggregate and concrete and volume ratio of mortar and concrete of mix-proportioning 3 is respectively shown in Fig 3.12 (a) and (b).

However, the same tendency as in mix-proportioning 1 and mix-proportioning 2 was not able to be observed in mix-proportioning 3.

The high viscosity of SCC using mix-proportioning 3 led to hard flow of concrete in the steel trough. The fall of concrete from V-funnel to the steel trough already cause the change of distribution of coarse aggregate and mortar in concrete. These lead to the weight ratio of coarse aggregate and concrete and volume ratio of mortar and concrete of mix-proportioning 3 exhibit disorderly and unsystematic tendency.

Table3.5 reveals the comparison of thickness of mortar adhering on the inner surface of steel trough. The thickness of mortar which adhered to the steel plate surface is around 1.4mm to1.5mm.

Fig 3.8 V-funnel Attached with Mortar

Fig 3.9 Steel Trough after Concrete Passed

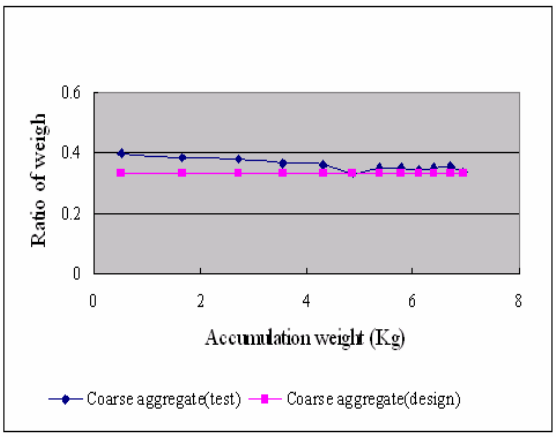

(a) Coarse Aggregate

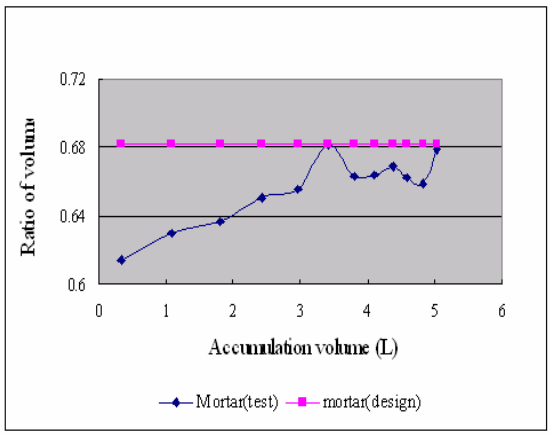

(b) Mortar

Fig3.10 Weight Ratio of Coarse Aggregate and Volume Ratio of Mortar of Mix-proportioning 1

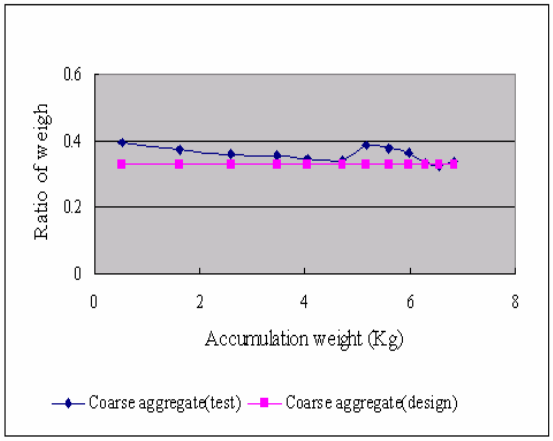

(a) Coarse Aggregate

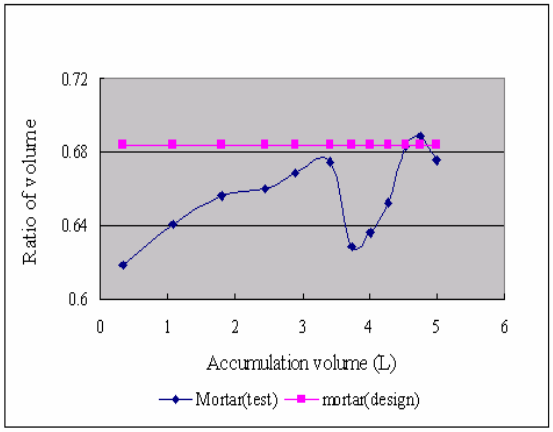

(b) Mortar

Fig3.11 Weight Ratio of Coarse Aggregate and Volume Ratio of Mortar of Mix-proportioning 2

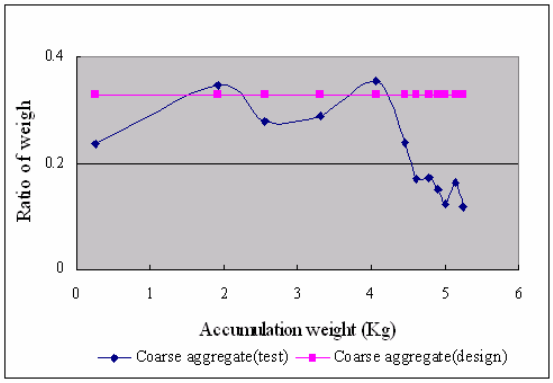

(a) Coarse Aggregate

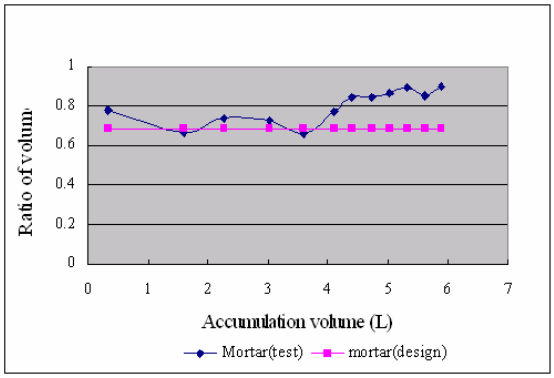

(b) Mortar

Fig3.12 Weight Ratio of Coarse Aggregate and Volume Ratio of Mortar of Mix-proportioning 3

Table3.5 Comparison of Thickness of Mortar Adhering on the Inner Surface of Steel Trough

	mix-proportioning 1	mix-proportioning 2	mix-proportioning 3
V-funnel time (sec.)	9	12	30
Slump flow (mm)	622 ×640	650 ×645	640 ×596
Density of concrete (Kg/m^3)	2488	2502	2511
Density of original Mortar (Kg/m^3)	2440	2451	2459
Thickness of mortar adhered in trough (mm)	1.447	1.469	-------

3.4 Conclusions

The following conclusions were made basing on the analyses and experimental work in this part of research program:

1) Concrete can be poured through several input ports only made on several columns and more than one story frame can be constructed using the new developed bottom up pumping method. The employ of branch pipe in this construction method also can decrease the number of pump car. Therefore, compared with the exited bottom up pumping method for CFT column-Steel frame structure, the new construction method for the new CFT column-CFT beam frame structure is supposed to be an efficient and cost-effective method.

2) Experiment on thickness of mortar which adheres to steel plate surface simulated the concrete flow in beam. The experiment result reveals the fact that the property of concrete changed during the concrete flow period. Mortar volume ratio changed due to amount of mortar adhering to the steel plate surface until it arrived to the value of original design and kept stable.

   The thickness of mortar which adhered to the steel plate surface is around 1.4mm to1.5mm.

CHAPTER 4

INVESTIGATION OF THE NEW DEVELOPED BOTTOM UP PUMPING METHOD USING VISUAL MODEL OF FRESH CONCRETE

4.1 Introduction

Chapter3 present the idea of the new developed bottom up pumping method from viewpoint of practical application for a whole building.

In order to further understand the flow tendency of concrete in the real building, visual model of fresh concrete which is easy to be observed, was employed in this part of research program. Chapter 4 explains the simulation mechanism of this visual model of fresh concrete.

A scale subassembly which was made of acrylics plate was made and visual model of fresh concrete was poured inside the subassembly in order to simulate the real flow tendency of concrete in the steel tube of column and beam. The experimental program and result is also presented in chapter 4.

4.2 Visual Model of Fresh Concrete

4.2.1 Concept of Visual Model of Fresh Concrete

Visual model of fresh concrete is a kind of effective method to observe and make analysis on the concrete flow situation in the real steel tube.

In the visual model, fresh concrete is simulated through two phases, mortar phase and coarse aggregate phase. During the flow period, the distribution of coarse aggregate in visual model is able to be observed obviously since the mortar of visual model is transparent.

4.2.2 Properties of Visual Model of Fresh Concrete

The simulation of fresh concrete using mortar phase and coarse aggregate phase must take the properties of the materials which were used to establish the visual model into account.

The materials of the visual model which were selected to simulate the mortar and coarse aggregate should have the following properties:

(a) The material which is used to simulate the mortar in the visual model should have

higher transparence in order to make it possible to observe the flow tendency of coarse aggregate phase during the flow period.

(b) The segregation resistance capability of visual model should close to that of fresh concrete.

(c) Both the visual model and fresh concrete should have similar mix-proportioning.

Generally, segregation occurs during the concrete pouring period and curing period after pouring. The reason for the former is due to the segregation between mortar and coarse aggregate. The latter is due to the sinkage of coarse aggregate accompanying with the occurrence of bleeding. In this research work, fresh concrete was divided into two phase to be simulated, the research is from the viewpoint of concrete flow tendency in the steel tube, thus the segregation which occurs during the curing period is not within the research range of this research program.

Therefore, basing on the analysis of segregation mechanism of coarse aggregate and mortar of concrete model, one particle from coarse aggregate group is taken as a research object. Subsequently, considering the relative velocity between this particle and ambient mortar, the sinkage situation of this particle in mortar is decided.

In this case, the particle is subjected to the forces of particle gravity, viscosity resistance and flotage provide by mortar. The balance equation including all these forces is as the following:

$$\frac{4}{3}\pi r^3 \rho \frac{dv}{dt} = \frac{4}{3}\pi r^3 \rho g - 6\pi r \eta v - \frac{4}{3}\pi r^3 \rho_m g \qquad (1)$$

r : Radius of coarse aggregate (cm)
ρ : Density of coarse aggregate (g/cm^3)
ρ_m :Density of mortar (g/cm^3)
η : Viscosity coefficient of mortar ($dyne.sec/cm^2$)
g : Acceleration of gravity (cm/sec^2)

If $\frac{dv}{dt} = 0$, the final relative velocity is obtained.

$$V = \frac{2r^3 g(\rho - \rho_m)}{9\eta} \qquad (2)$$

From the equation (2), it reveal that the final relative velocity has the relationship with

the diameter of particle, the density difference of coarse aggregate and mortar and the viscosity of mortar.
Therefore, the following three conditions should be satisfied in order to make sure that the segregation resistance capability of visual model is close to the segregation resistance capability of fresh concrete.

(1).The diameter of coarse aggregate in visual model should be same as in fresh concrete, which means that the particle distribution of visual model and the maximum diameter of coarse aggregate in visual model are same as that in fresh concrete.

(2).Density difference between coarse aggregate and mortar of visual model should be same as that in fresh concrete. The density of the used material is calculated basing on the density of water at 4℃。 Therefore, if visual model and fresh concrete are disposed under same temperature, density difference can be considered instead of specific gravity difference of coarse aggregate and mortar, viz. the density difference of coarse aggregate and mortar of visual model should be same as that of fresh concrete.

(3) The viscosity of mortar phase of the visual model should similar as fresh concrete. According to the former research result on block mechanism of concrete flow in the steel tube, the volume ratio of coarse aggregate and mortar (V_g/V_m) is one of important factor that lead to the occurrence of block. Therefore, the volume ratio of coarse aggregate and mortar (V_g/V_m) of visual model should similar to that of fresh concrete. The decisions of distribution of coarse aggregate size, shape of coarse aggregate and the maximum size of coarse aggregate of visual model are also important.

4.2.3 Model of Mortar of Visual Model

The mortar model is made of water absorptivity high polymer resin, which is a kind of white powder, mixing with water. This mixture has properties of high viscosity and high transparency. Fig4.1 (a) shows the photo of water absorptivity high polymer resin.
Many materials can be used to make mortar model since they also has the properties of high viscosity and high transparency. The advantage of water absorptivity high polymer resin is that the properties of it are stable along with time, due to insensitively effecting by the ambient temperature and humidity. Furthermore, this material is easy to be obtained.
On the other hand, a relatively large amount of material is consumed in the simulation

of fresh concrete flow experiment using visual model. Mortar model made by water absorptivity high polymer resin mixing with water is able to be used repetitiously since their property is insensitive to the ambient circumstance, thus it can lead to decrease of labor work and cost.

After the experiment, the mortar model, viz. the mixture of water absorptivity high polymer resin and water can flow with tap water without need of special disposal, thus the coarse aggregate material can be recycled. Thus the coarse aggregate is also able to be reused, which can avoid the repetitious preparation works for material.

As the above explanation, it has many advantages using water absorptivity high polymer resin solution to serve as mortar model in visual model. Thus, the problem that the material properties should change along with time is solved by using this method. The properties of water absorptivity high polymer resin is shown as Table4.1

Table 4.1 Properties of Water Asorptivity High Polymer Resin

Absorption (g/g)				PH	Density (g/ml)	Moisture Ratio (%)	Particle Distribution (Weight %)		
Deoxyg-enated water	Normal saline	1.8% saline	Sheep blood				>20 mesh	20 mesh	<20 mesh
700	65	50	70	neutrality	0.4	<7	1	89	10

The material properties results reveal that the dosage of water absorptivity high polymer resin in 1liter water is one of the essential factors which affect the viscosity of water absorptivity high polymer resin solution. The effect of the dosage will be explained in detail in section 4.3.1.

Among three conditions should be satisfied in order to make sure that the segregation resistance capability of visual model is similar to that of fresh concrete, as the third condition explained, considering the importance of viscosity effect of mortar to the concrete, the viscosity of mortar model in visual model should have replacement capability with viscosity of fresh concrete.

The proposed mortar model makes it possible to simulate the different kinds of concrete with different viscosity, which affects the occurrence of segregation between coarse aggregate and mortar.

Furthermore, tap water is employed in making the mortar model in visual model, thus make it unnecessary to consider about the effect of temperature to properties of mortar model. It can be considered that the viscosity of mortar model keep constant along with

time.

4.2.4 Model of Coarse Aggregate of Visual Model

The specific gravity of coarse aggregate which is employed in fresh concrete is around 2.6. The specific gravity of the former proposed mortar is around 1.0. If coarse aggregate which is used in fresh concrete is employed in visual model and mixed with the proposed mortar model, the significant effect of specific gravity will lead to high segregation occurrence probability compared with that of fresh concrete. The problem can not be solved even by increasing the viscosity of mortar model.

Form the viewpoint of fresh concrete, the difference of specific gravity between coarse aggregate and mortar is around 0.3. In order to ensure that the segregation resistance capability of visual model is similar as that of fresh concrete, the proposed coarse aggregate in visual model should approximately has specific gravity of 1.3.

Basing on the former analysis, it is suitable to select artificial lightweight coarse aggregate to serve as coarse aggregate model in visual model due to the satisfaction of its specific gravity value. Fig4.1 (b) shows photo of artificial lightweight coarse aggregate.

Many materials have similar shape to sand and crush stone. Whereas, form the viewpoint of specific gravity of 1.3, cost and available possibility of these materials, artificial lightweight coarse aggregate is more suitable then others to be used as coarse aggregate model in visual model.

(a) Water Absorptivity High Polymer Resin

(b) Artificial Light Weight Coarse Aggregate

Fig4.1 Model of Visual Model

The diameter of artificial lightweight coarse aggregate is between 5~15mm, this is also

an advantage in the concrete flow simulation experiment, which will be present in detail in section 4.3.1.

4.3 Experimental Work of Simulation of Fresh Concrete Flow Using Visual Model

In the concrete flow simulation experimental research work, totally two experiment projects were conducted. One experiment project is simulating flow tendency of fresh concrete with superior properties. The other one is simulating flow tendency of fresh concrete with inferior properties.

4.3.1 Test Setup and Material Property

A scale subassembly which is made of acrylics plate was employed in this experiment. Fig4.2 (a) schematically shows the three-dimensional image of the subassembly, Fig4.2 (b) shows dimensions of the subassembly.

Artificial lightweight coarse aggregate

As explained in former sections, coarse aggregation phase of visual model is made of artificial lightweight coarse aggregate. The diameter of coarse aggregate which is used in fresh concrete is 5mm~25mm. In this experimental work, however, a scale subassembly is employed, thus the diameter of artificial lightweight coarse aggregate is limited to 5mm~10mm.

The artificial lightweight coarse aggregate is immerged into the water for 24 hours before used. The specific gravity of saturated-surface-dry (SSD) situation of it is 1.72.

Solid volume of the artificial lightweight coarse aggregate is 60.5%.

Water absorptivity high polymer resin

Mortar model of visual model is made of water absorptivity high polymer resin mixing with water. According to the experimental result, the flowability and viscosity of the water absorptivity high polymer resin solution is primarily affected by two factors, mixing time and dosage of polymer resin add in 1liter water. Table 4.2 shows some information about this effect.

4.3.2 Test Program

Mixing program of visual model was different form that of fresh concrete. The artificial lightweight coarse aggregate was crushed by mixer which is used for mixing fresh

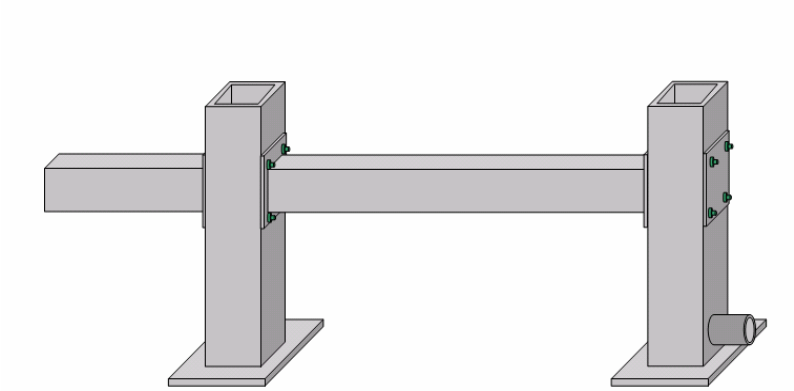

(a)

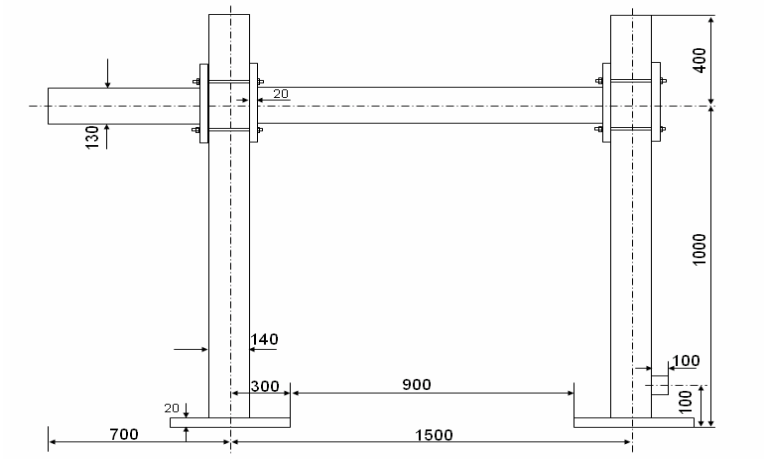

(b)

Fig4.2 1/4 Scale Subassembly

Table 4.2 Affect of Mixing Time and Dosage of Polymer Resin to the Flowability and Viscosity of Solution

Water absorptivity high polymer resin (g/l)	Mixing Time (min.)	Slump Flow (mm)	V-funnel Time (sec.)
3	6	190×185	3
3.5	4	190×189	4
4	3	187×185	7
4	4	158×156	14
4	5	160×156	19
4.5	4	167×170	20

concrete. In order to obtain expected visual model, firstly water absorptivity high

polymer resin was mixed with water by the mixer which was specially used for mortar mixing; subsequently, the obtained mortar model was mixed with artificial lightweight coarse aggregate by hand. Totally 60 liter visual model of fresh concrete is needed. Due to the limitation of capacity of mortar mixer, 15liter of visual model is mixed in each mixing period and totally 4 mixing periods are needed. The 4 mixing periods lasted for nearly 1 hour from the beginning to the end.

After the total 60 liter visual model was obtained, slump flow test and v-funnel test were conducted.

Finally, the visual model of fresh concrete was poured into the acrylics subassembly from a higher position through a 3 meter plastic hose which was tied to the barrier of stair. A typical test setup is shown in Fig 4.3.

Fig4.3 Typical Test Setup for Concrete Flow Simulation Using Visual Model of Fresh Concrete

4.3.3 Simulation of Flow Tendency of Fresh Concrete with Superior Properties

In this experiment project, 4 minutes mixing time was selected for mortar mixing; 4.5g/L dosage was selected in visual model mix-proportioning, which is shown in Table 4.3.

Fig 4.4 shows the photo of slump flow test. The slump flow was 430mm×445mm and

V-funnel is 8 sec.

Table 4.3 Mix-proportioning of Visual Model in Project Ⅰ (kg/m^3)

Water absorptivity high polymer resin (g/l)	Artificial lightweight coarse aggregate	Water absorptivity high polymer resin	Water
4.5	519.72	3.09	687.27

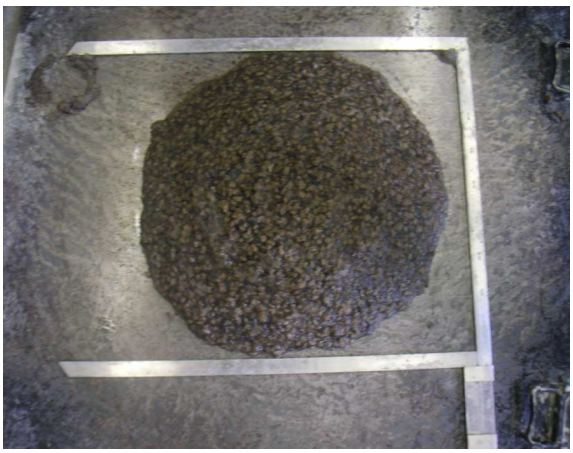

Fig 4.4 Slump Flow Test of Visual Model in Project Ⅰ

During the whole construction period, the visual model of fresh concrete flowed form plastic hose to the bottom of acrylics subassembly, then arrived to the top of the acrylics column tube; subsequently, it flowed to the second acrylics column through the horizontal acrylics beam, dropped from top to the bottom of the column; finally, the visual model of fresh concrete arrived to the top of the second acrylics column again and flowed out of the acrylic subassembly through the second parts of beam.

The whole flow process of visual model was smooth and continuous. Coarse aggregate phase and mortar phase kept good combination situation from the beginning to the end of the flow process except at the position of connection panel, where the visual model exhibit a little bit of segregation. However, drop of visual model form top to the bottom of acrylics column did not lead to the occurrence of segregation. Fig4.5 shows the situation that visual model flow in different position of subassembly in experiment project Ⅰ.

(a) Bottom of First Column

(b) Middle of First Column

(c) First Connection Panel

(d) Beam Between two Columns

(e) Second Connection Panel

(f) Bottom of Second Column

(g) Second Connection Panel

(h) Second Part of Beam

Fig4.5 Visual Model Flow in Different Position of Subassembly in Project Ⅰ

Fig4.3 shows the situation of the whole subassembly after pouring concrete in experiment project Ⅰ.

The result that visual model of fresh concrete is able to flow through the whole acrylics subassembly successfully indicate that possibility of fresh concrete being constructed to the building frame by the new developed bottom up pumping method.

4.3.4 Simulation of Flow Tendency of Fresh Concrete with Inferior Properties

In this experiment project, 6 minutes mixing time was selected for mortar mixing; 3g/L dosage was selected in visual model mix-proportioning, which is shown in Table 4.4.

Fig 4.6 shows the photo of slump flow test. The slump flow was 660mm×640mm and V-funnel is 2 sec.

Table 4.4 Mix-proportioning of Visual Model in Project Ⅱ (kg/m^3)

Water absorptivity high polymer resin (g/l)	Artificial lightweight coarse aggregate	Water absorptivity high polymer resin	Water
3	519.72	2.07	689.83

Fig 4.6 Slump Flow Test of Visual Model in Project Ⅱ

In the experiment project Ⅱ, the experiment was conducted by two times. In the first time experiment, a relative low pouring speed was employed. The visual model of fresh concrete flowed form plastic hose to the bottom of acrylics subassembly, however, it could not arrive to the first connection panel due to the premature occurrence of block

in the plastic hose and position around input port which locates at the bottom of the first column. The low viscosity of mortar in visual model make it impossible to let the coarse aggregate be taken to flow together with mortar, thus lead to most of mortar in visual model flowed faster than coarse aggregate, these cause the premature occurrence of block. The experiment had to be terminated.

In the second time experiment, the pouring speed was increased in order to avoid the premature occurrence of block.

The visual model of fresh concrete flowed form plastic hose to the bottom of acrylics then arrived to the top of the acrylics tube; segregation between mortar and coarse aggregate already occurred during this period, thus mortar flowed to the second acrylics column through the horizontal acrylics beam, dropped from top to the bottom of the column before coarse aggregate; then a part of coarse aggregate was taken by mortar passing through the horizontal acrylics beam and dropping from top to the bottom of the column. Coarse aggregate then sink and concentrated to the bottom of the second acrylics column; finally, the mortar of visual model arrived to the top of the second acrylics column again and flowed to the second parts of beam.

Ultimately, the mortar of visual model could not flow out of the subassembly through the second parts of beam due to the occurrence of block.

Before the occurrence of block, the whole flow process of visual model was relatively smooth and continuous. However, segregation between coarse aggregate phase and mortar phase was occurred soon after the visual model arrived to the bottom of first acrylics column, the two phase could not keep good combination situation from the beginning to the end of the flow process, coarse aggregate concentrated to the bottoms of the two acrylics columns while mortar concentrated to the tops of the two acrylics columns.

Fig4.7 shows the situation that visual model flow in different position of subassembly in experiment project Ⅱ. Fig4.8 shows the situation of the whole subassembly after pouring concrete in experiment project Ⅱ. Fig 4.9 shows the block situation in the plastic hose.

The result that visual model of fresh concrete is unable to flow through the whole acrylics subassembly successfully in the second experiment project indicate that block can easily occur due to the inferior properties of fresh concrete in the really construction practice.

(a) Bottom of First Column

(b) Middle of First Column

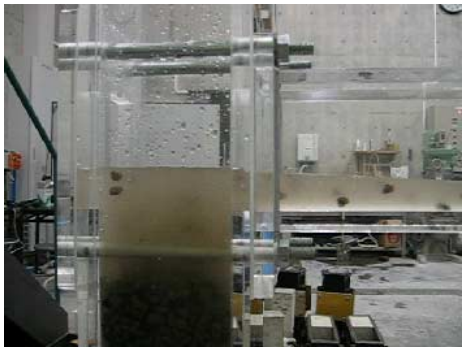

(c) First Connection Panel

(d) Beam Between two Columns

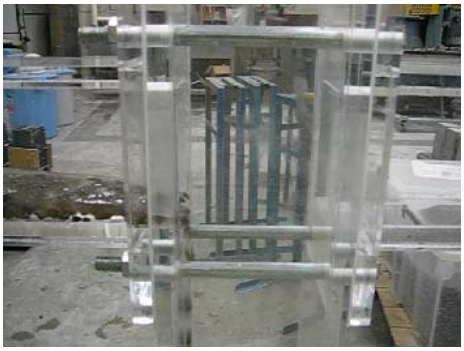

(e) Second Connection Panel

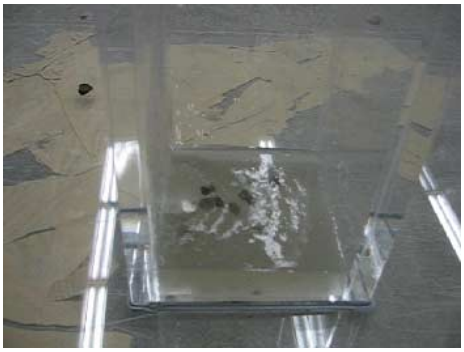

(f) Bottom of Second Column

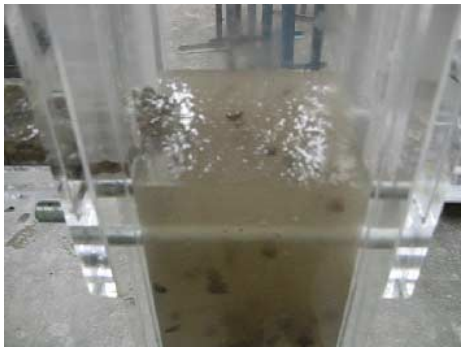

(g) Second Connection Panel

(h) Second Part of Beam

Fig4.7 Visual Model Flow in Different Position of Subassembly in Project Ⅱ

Fig4.8 Situation of the Whole Subassembly after Pouring Concrete in Experiment Project Ⅱ

Fig4.9 Block Situation in Plastic Hose

4.4 Conclusions

1) The proposed new developed bottom up pumping method for the new CFT column-CFT beam frame structure in chapter 4 can be simulated by the visual model of fresh concrete. The flow tendency of concrete in column-beam subassembly is able to be observed obviously. The proposed construction method is supposed to be feasible to be applied on condition that the fresh concrete has prior properties.

2) The experimental work also revealed that block may easily occur due to the inferior properties of fresh concrete. The compaction quality will be strongly affected due to the segregation occurrence between coarse aggregate and mortar. Pouring speed also effect the construction result. Lower pouring speed led to earlier occurrence of block than higher pouring speed.

CHAPTER 5

BUILDING FRAME DESIGN AND COST PERFORMANCE ANALYSIS

5.1 Introduction

This chapter presents the overview on the design of 9, 18 and 40-story unbraced building frames made of both CFT column-CFT beam frame structure and conventional hollow steel tube-H beam steel structure. Inelastic analysis was conducted using the structure analysis software STAAD.Pro, which is popularly used for structural analysis and design. In this part of research work, firstly the behavior of each frame, both new CFT column-CFT beam structure frame and conventional steel structure frame, under combination of seismic load were analyzed thus to obtain the strength and ductility demand at different locations in the building. Subsequently, the dimension of each component member of each frame was decided according to the analysis results. Finally, the cost of each frame was calculated and compared basing on the former decided dimensions of component members.

5.2 Trial Design of Building Frame

5.2.1 General description of theme structures

Theme structures treated in this research are 9, 18 and 40-story unbraced building frames of office made of CFT column-CFT beam frame system and conventional steel frame system. Fig5.1 shows a typical framing elevation of the three different story office buildings. A typical floor plan is shown in Fig5.2, which is common for all six theme structures designed. For CFT column-CFT beam structure system, square cross section CFT structure is used for columns and rectangle cross section CFT structure is used for beam; for steel structure, hollow steel tube with square cross section is used for columns and H-shaped steel is used for beams. Different elevations of a 9-story building along two directions are shown in Fig5.3 and Fig5.4 respectively. The height of each typical story is 3.8m, resulting in a total height of 34.2m, 68.4m and 152m for 9, 18 and 40-story building respectively. Total plan dimensions for each building are 28.4×36.0m. There are no vertical or horizontal irregularities in the buildings.

As show in Fig5.2, the structure is composed of four frames in the X-direction along lines 1, 2, 3, and 4, and seven frames in the Y-direction along lines A to G.

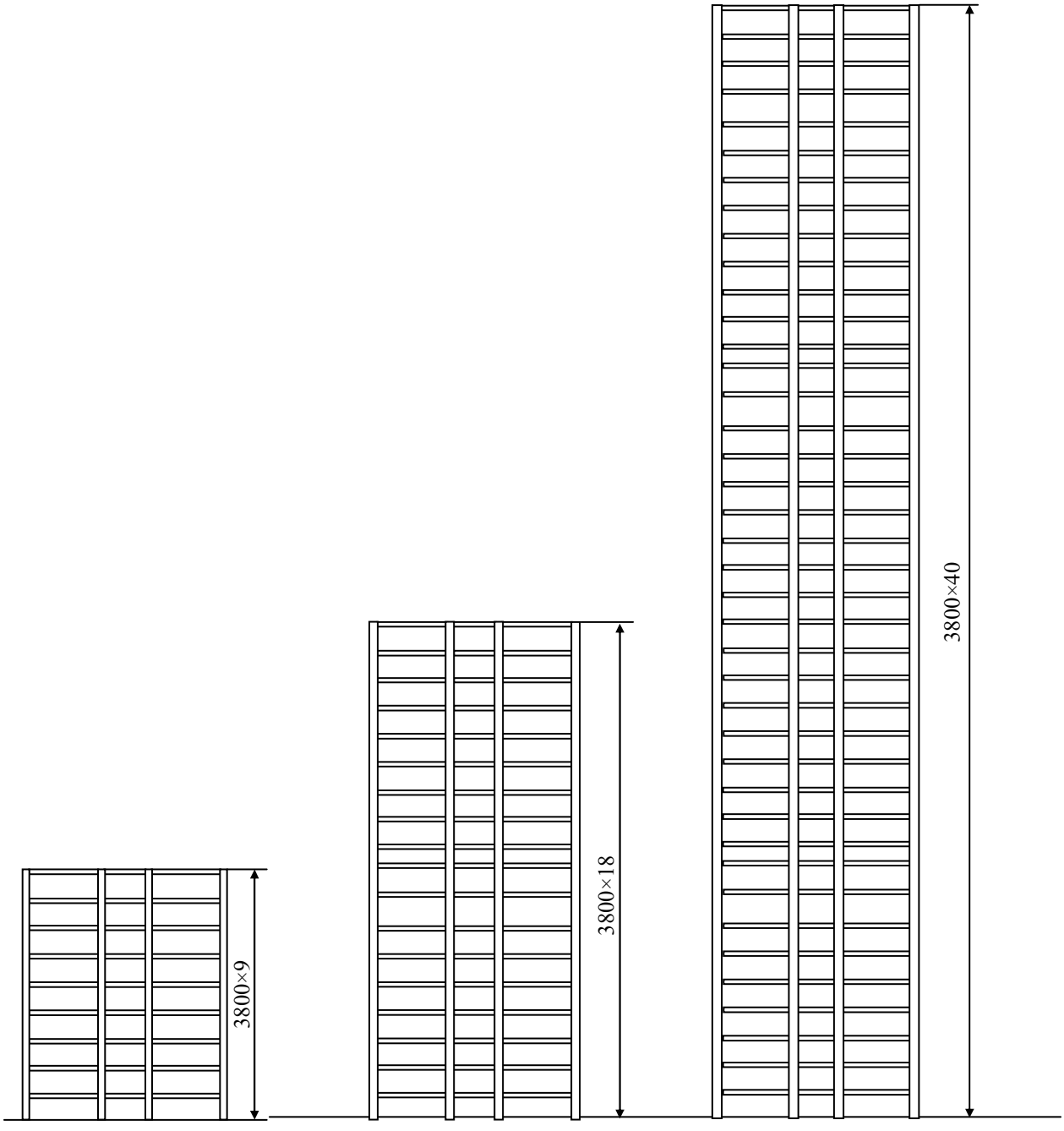

Fig5.1 Framing Elevation

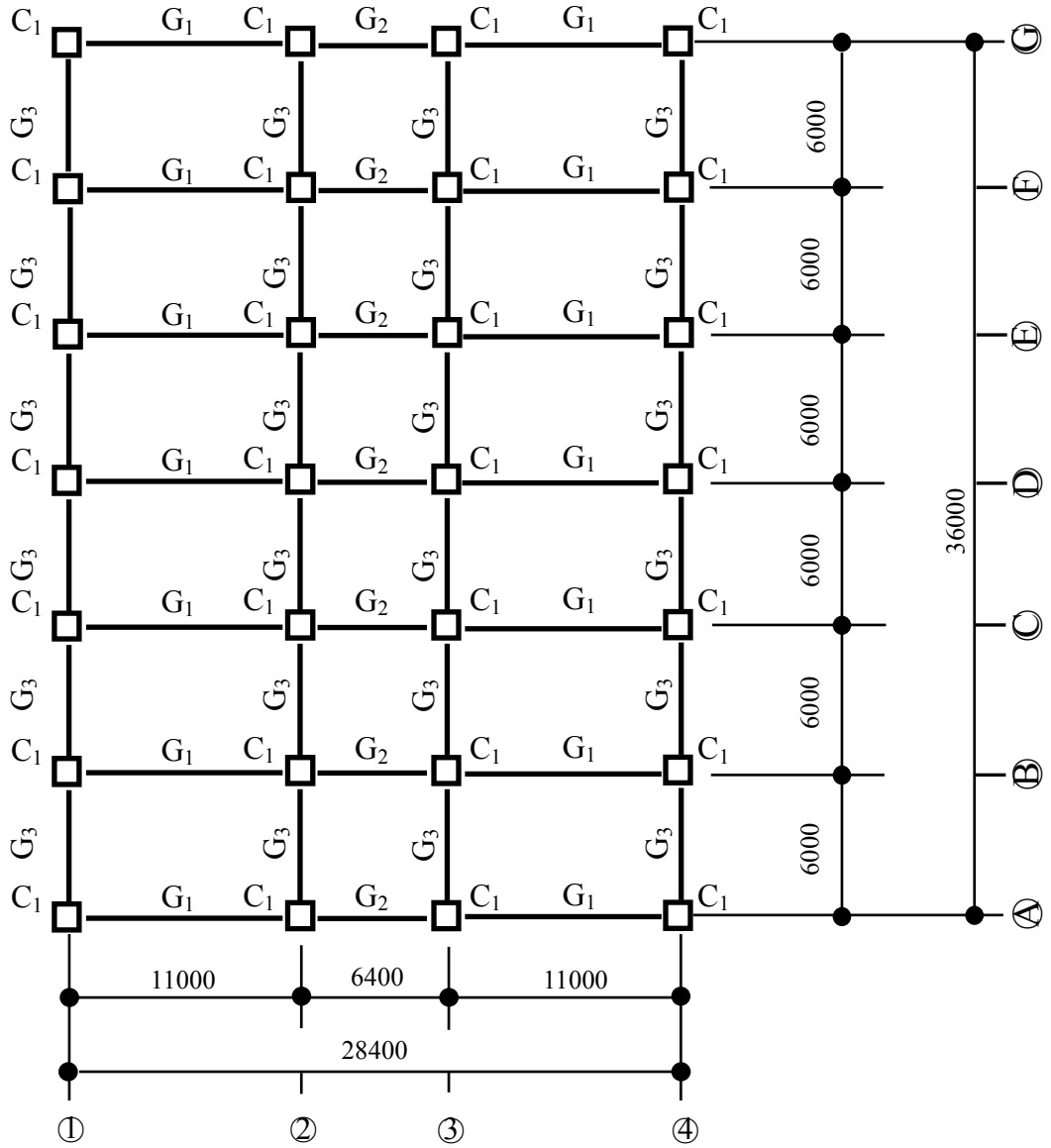

Fig5.2 Framing Floor Plan

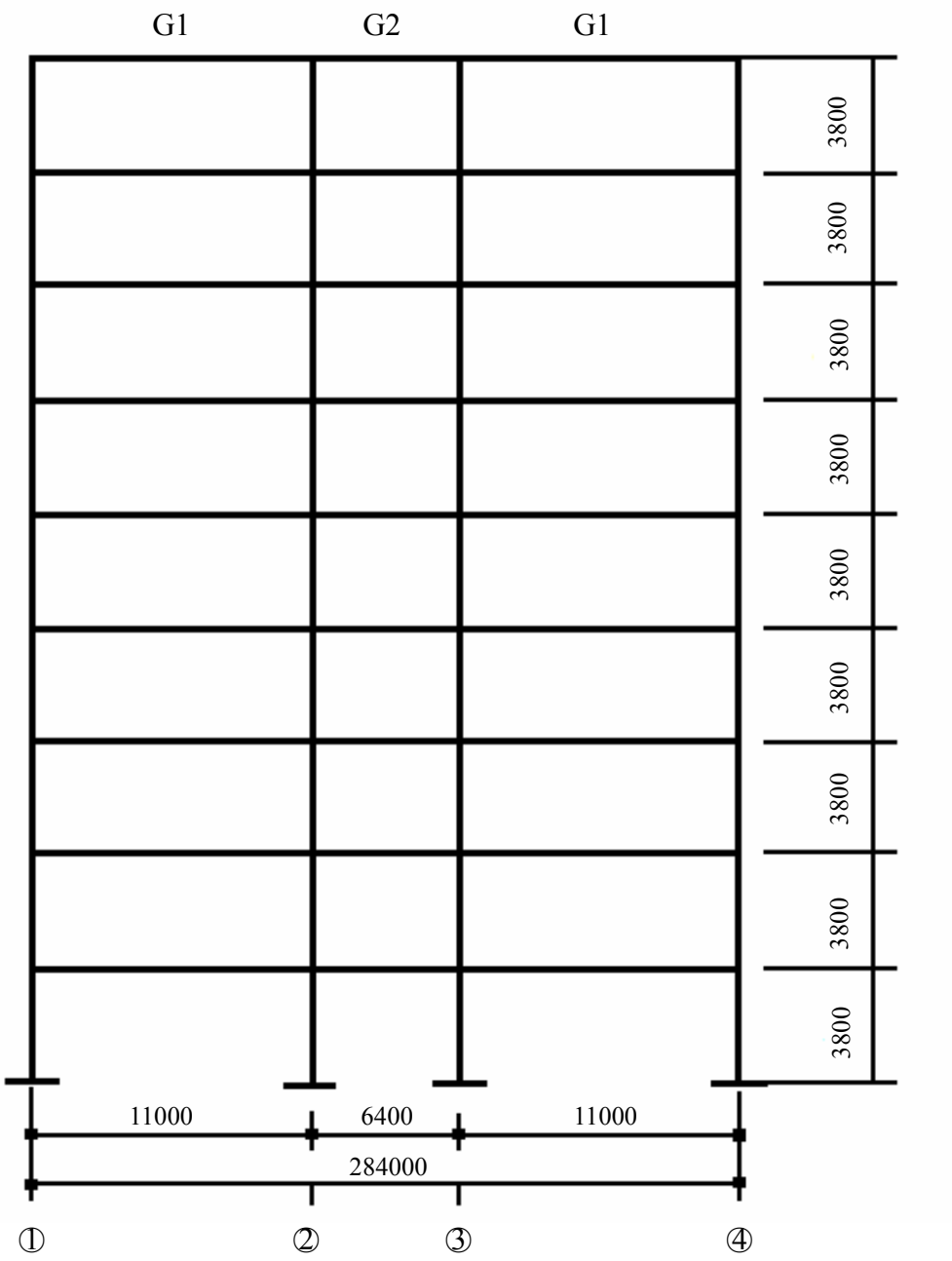

Fig5.3 Elevation of Frame C of 9-story Building

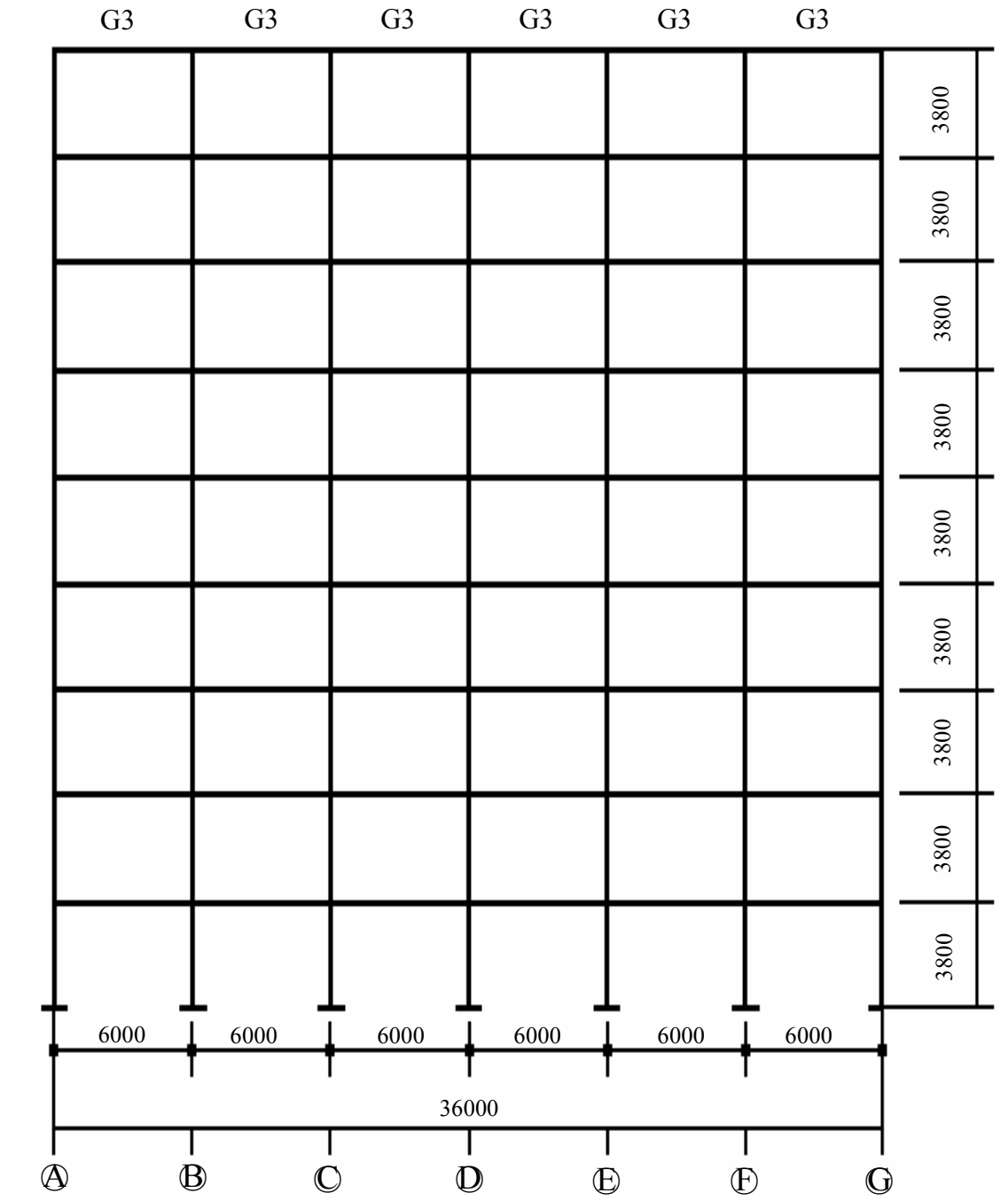

Fig5.4 Elevation of Frame 3 of 9-story Building

The steel structural design is mainly based on Specification for Structural Steel Design of Japan and the CFT structural design is mainly based on Recommendations for Design and Construction of Concrete Filled Steel Tubular Structure. All connections are assumed to be rigid connections. No bracing or shear walls are used in the structure. Concrete compressive strength, f_c is 80MPa while the steel yield strength, f_y is 235Mpa. All frames were designed by the allowable stress design against the seismic shear force under earthquake. In the course of design, each member was proportioned in such a way that the plastic hinges mainly formed in beams, and the columns remained elastic until the mechanism state was reached.

5.2.2 Load Conditions

Dead Load and live load were taken according to Recommendations for Loads on Buildings (AIJ 1993 revision). Load cases which were taken into account including dead load W_D, Live load W_L, Wind load W_W and Seismic load W_E. Table 5.1 shows the intensities of gravity loads, which are normally employed in the design practice of a typical office building in Japan. The structure is assumed to locate in Osaka where the wind speed of this wind zone is 36m/s.

Totally four load combinations were taken into account as the following:

Dead load + Live load	$1.0W_D+1.0W_L$
Dead load + Wind Load+ Live load	$1.0W_D+0.8W_W+0.6W_L$
Dead load + Seismic Load+ Live load	$1.0W_D+0.3W_E+0.4W_L$

Table5.1 Design Loads

	Dead load (N/m^2)	**Live load (N/m^2)**	
		For vertical	**For seismic**
Roof	3800	1000	300
Office	2700	1600	700

5.2.3 Design Conditions

In a conventional seismic design of a building structure, the concept of weak beam and strong column has been adopted to avoid energy concentration to a specific story. Thus, the following design conditions were adopted in this design: The ratio of the stress in the column caused by the design load to the allowable stress was kept as near to 0.8 as possible and that of the beam as near to 1.0 as possible; story drift angles were kept within about 1/200 under the design load in the design and the collapse mechanism at the ultimate state was the overall frame mechanism in which the plastic hinges formed only in beams, and all columns remained elastic.

5.2.4 Members Design

In this design research, firstly the steel structure of 9, 18 and 40-story building was designed according to the AIJ steel structure design code thus the dimensions of steel members were decided; then, based on the load distribution on each steel member of the building, the dimensions of CFT members were firstly chosen roughly. Each CFT member which was chosen has similar or close to load capacity or moment capacity as the corresponding steel member; subsequently, the construction analysis of the whole CFT structure building was conducted. The story drift angle of each story both in steel structure building and CFT structure building was compared; readjusting the dimensions of partial unsuitable CFT members and making analysis for the whole CFT building again until the story drift angle of CFT structure building closed to the steel structure; finally, checking the load distribution situation of each member and verifying that the strength of each story exceeded the required value. Thus the dimensions of CFT members were confirmed ultimately.

5.2.5 Building frame design of 9-story office building

As the design steps described above, two 9-story office building frames both using conventional steel structure and CFT column-CFT beam structure respectively were designed firstly by structure analysis software STAAD.Pro.

Fig5.5 to Fig 5.7 serves as the examples to show how to check whether the selected CFT member strength is sufficiently for the building design. Fig5.5 is the example to show checking the column members in story 6 of the 9-story building along X-direction. In Fig5.5 (a), the envelope curve represents the axial load and moment relationship of the selected CFT member. The four points inside the curve represent the load distribution values on four CFT column members along X-direction in the building of story 6 under the design combined seismic load. The situation that all these four points

inside the envelope curve reveals that the selected CFT member is sufficient for the CFT structure building frame along X-direction in story 6. In Fig5.5 (b), the two envelop curves represent axial load and moment relationship of the selected CFT member and the selected steel member respectively. The four points inside the curve represent the load distribution values on four steel column members along X-direction in the building of story 6 under the design combined seismic load. The situation that the four points inside both cures reveal that both of the selected CFT member and steel member is sufficient for the steel structure building frame along X-direction in story 6.

Fig5.6 is the example to show checking the column members in story 6 of the 9-story building along Y-direction. In Fig 5.6 (a), the total six CFT column members along Y-direction are all inside the axial load and moment relationship envelope curve of the selected CFT members; in Fig 5.6 (b), the total six steel column members along Y-direction are all inside the axial load and moment relationship envelope curves of the selected CFT members and steel members, which indicate that the sufficiency of selected CFT column members along Y-direction in the building of story 6 under the design combined seismic load.

Fig5.7 is the example to show checking the beam members in story 4 of the 9-story building along Y-direction. The situation that all the beam members point both in Fig5.7 (a) and Fig 5.7 (b), which represent the CFT structure members and steel structure members respectively, all inside the envelop curve of selected CFT member indicates the sufficiency of selected CFT beam members along Y-direction in the building of story 4 under the design combined seismic load.

Therefore, all the CFT column members and CFT beam members were checking to be sufficient for the building frame design using this method.

Table 5.2 shows the list of column members for 9-story building frame both in steel structure and CFT structure. The list of beam members both in steel structure and CFT structure is shown as Table 5.3. The comparison between the steel structure members and CFT structure members indicated that for column members, the areas of steel tubes of CFT columns are approximately 60~70% of that steel structure. Whereas, the yield moment of steel column members are approximately 100~130% of that steel column members. Compared with steel structure column members, partial CFT column members have same dimensions as steel structure while the thickness of steel tube decreased; partial CFT column members decrease both in dimensions and thickness of steel tube.

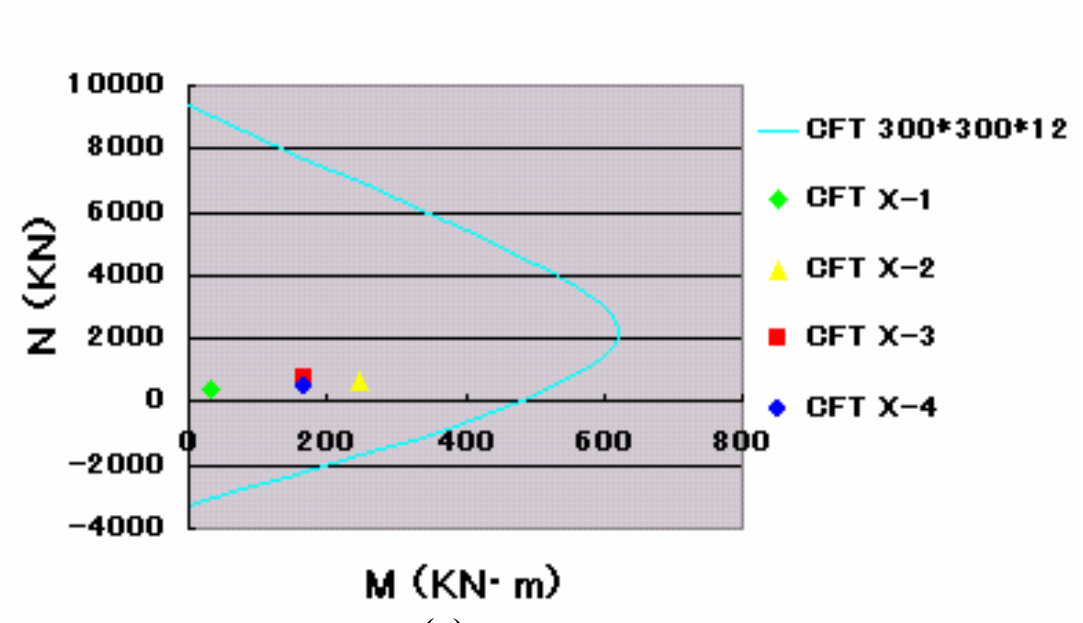

(a)

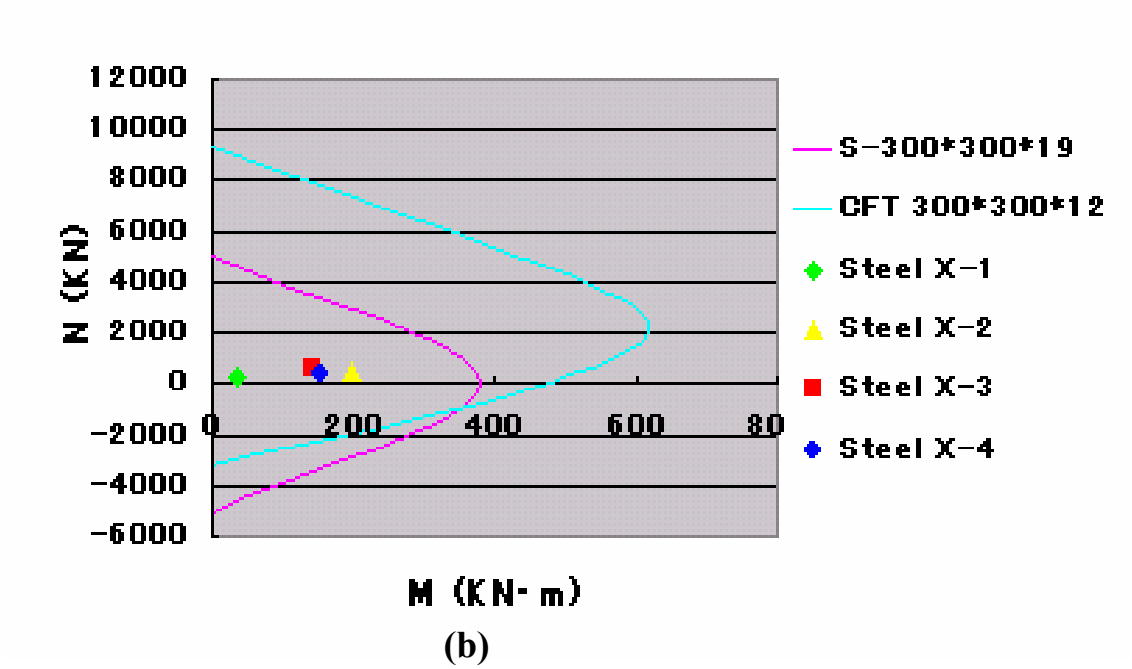

(b)

Fig 5.5 M-N Relationship of Column Member in Story 6 of 9-story Building X-direction

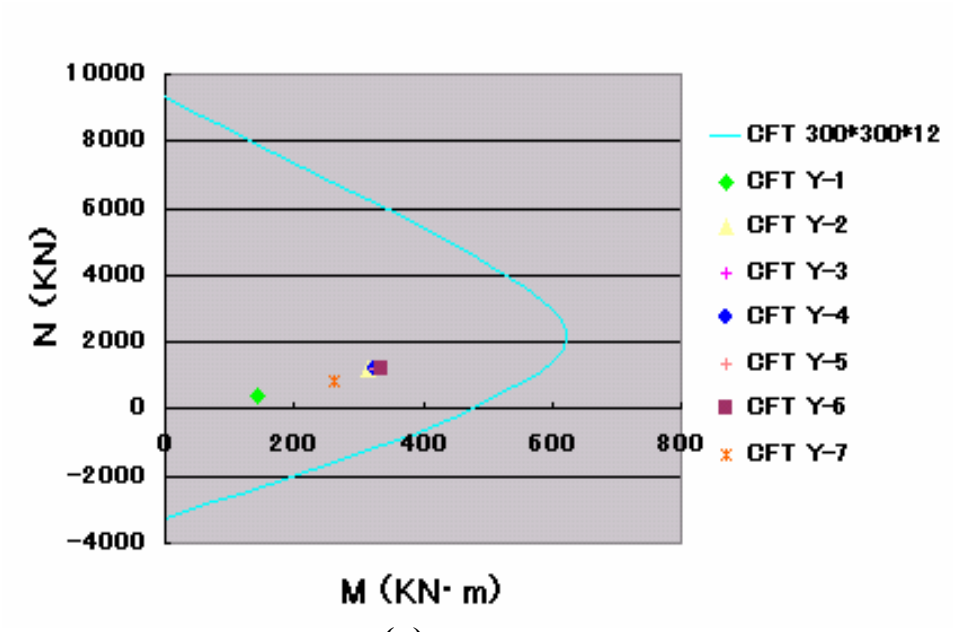

(a)

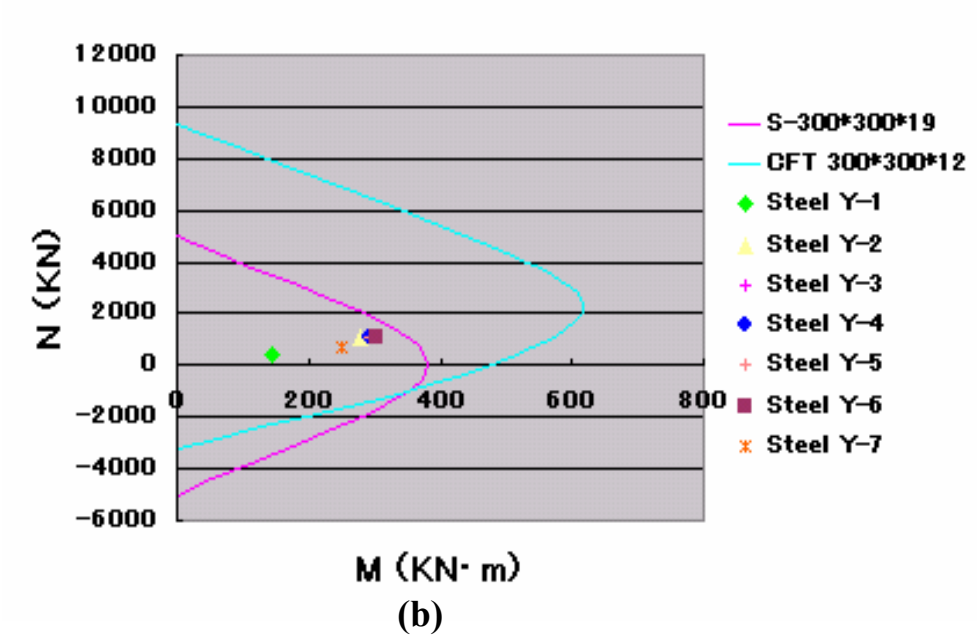

(b)

Fig 5.6 M-N Relationship of Column Member in Story 6 of 9-story Building Y-direction

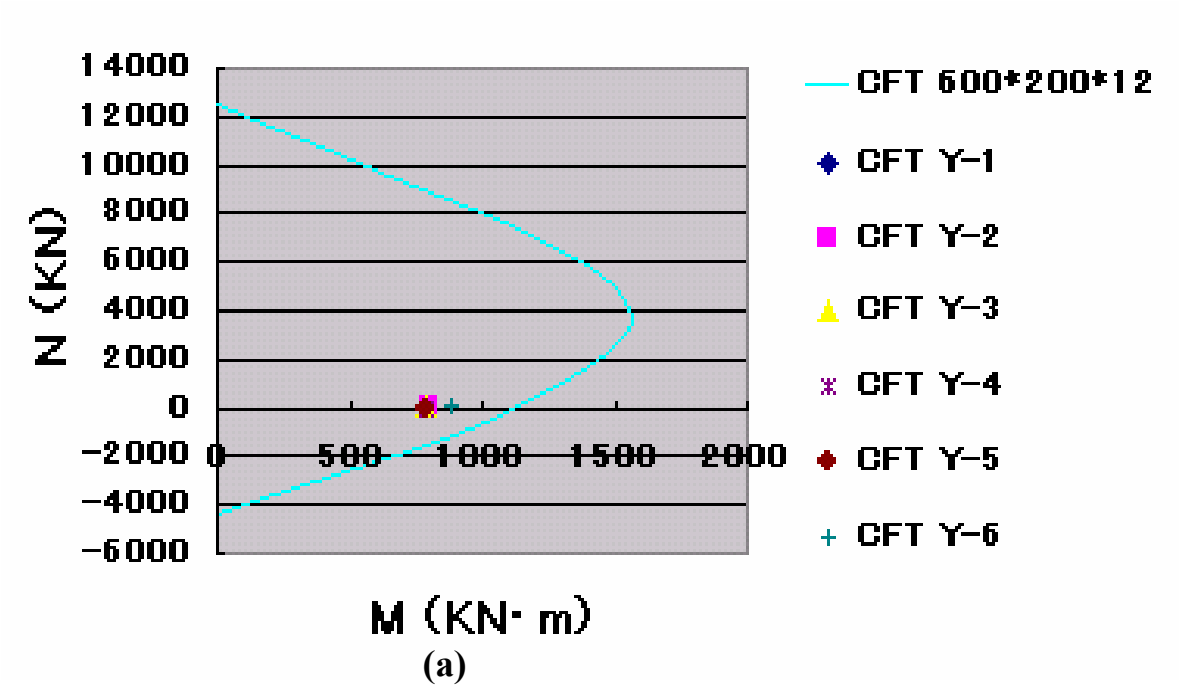

(a)

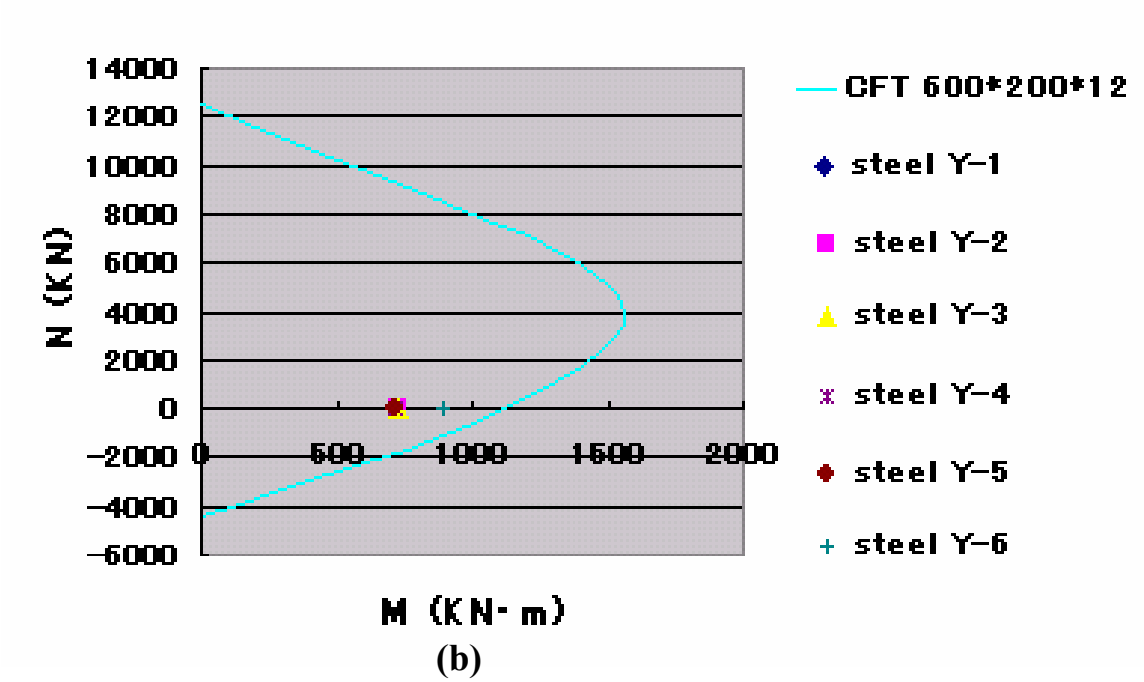

(b)

Fig 5.7 M-N Relationship of Beam Member in Story 4 of 9-story Building Y-direction

In the case of beam members, the areas of steel tubes of CFT beams are approximately 50~80% of that steel structure and the yield moment of steel beam members are approximately 60~80% of that steel beam members.

Table5.2 Column Members List of Steel and CFT Structure of 9-story Building

	Steel structure			CFT structure		
Story	**Dimension (mm)**	**M_u (kN·m)**	**A_s (cm^2)**	**Dimension (mm)**	**M_u (kN·m)**	**A_s (cm^2)**
8-9	□-300×300×9	244	105	□-250×250×6	230	59
6-7	□-300×300×19	381	232	□-300×300×12	480	138
4-5	□-400×400×19	741	290	□-350×350×16	850	214
2-3	□-450×450×25	1138	425	□-450×450×16	1410	278
1	□-550×550×25	1820	525	□-550×550×16	2114	342

Table5.3 Beam Members List of Steel and CFT Structure of 9-story Building

	Steel structure			CFT structure		
Story	**Dimension (mm)**	**M_u (kN·m)**	**A_s (cm^2)**	**Dimension (mm)**	**M_u (kN·m)**	**A_s (cm^2)**
9-7	H-390×300×10	457	133	□-400×200×6	335	70
6-5	H-582×300×12	790	169	□-450×150×12	574	138
4-1	H-692×300×13	1141	208	□-600×200×9	899	141
9-7	H-600×200×11	592	132	□-400×200×6	335	70
6-5	H-692×300×13	1141	208	□-600×200×9	899	141
4-3	H-792×300×14	1472	240	□-600×200×12	1123	186
2-1	H-900×300×16	2110	306	□-650×300×12	1563	222

For serviceability requirements, the structure is designed to have a limited story drift under design loads. The story drift angle is the difference between the deflections at the top and the bottom of the story divided by the height of that story. In the building frame design, all the story drift angles of are limited to within 1/200. Table 5.4 shows the story drift angle values of CFT column-CFT beam frame structure and steel frame structure

under design combined seismic load. All the story drift angle values of the design building are within 1/200. The comparison result of two kinds of structure indicates that CFT column-CFT beam frame structure has nearly same or even a little bit smaller value than steel structure which means despite increase the dead weight, the employment of CFT structure to the beam is able to increase the stiffness of the whole structure.

Table5.4 Story Drift Angles of Steel and CFT Structure of 9-story Building under Seismic Load

Story	CFT		S		CFT/S	
	X	Y	X	Y	X	Y
9	1/292	1/292	1/287	1/293	0.98	1.0
8	1/276	1/278	1/269	1/277	0.97	0.99
7	1/276	1/287	1/266	1/280	0.96	0.98
6	1/275	1/285	1/260	1/276	0.95	0.97
5	1/284	1/290	1/267	1/281	0.94	0.97
4	1/292	1/298	1/276	1/292	0.95	0.98
3	1/313	1/342	1/319	1/333	1.02	0.97
2	1/340	1/363	1/332	1/348	0.98	0.96
1	1/462	1/439	1/419	1/456	0.91	1.04

5.2.6 Building frame design of 18-story office building

In order to investigate the advantage of the new CFT column-CFT beam frame structure in high-rise building, an 18-story office building frame were designed. The design and checking method is same as 9-story office building design described above.

Fig5.8 is the example to show checking the column members in story 9 of the 18-story building along X-direction. Fig5.9 is the example to show checking the column members in story 9 of the 18-story building along Y-direction. One example to show checking the beam members in story 4 of the 18-story building along Y-direction is shown as Fig5.10.

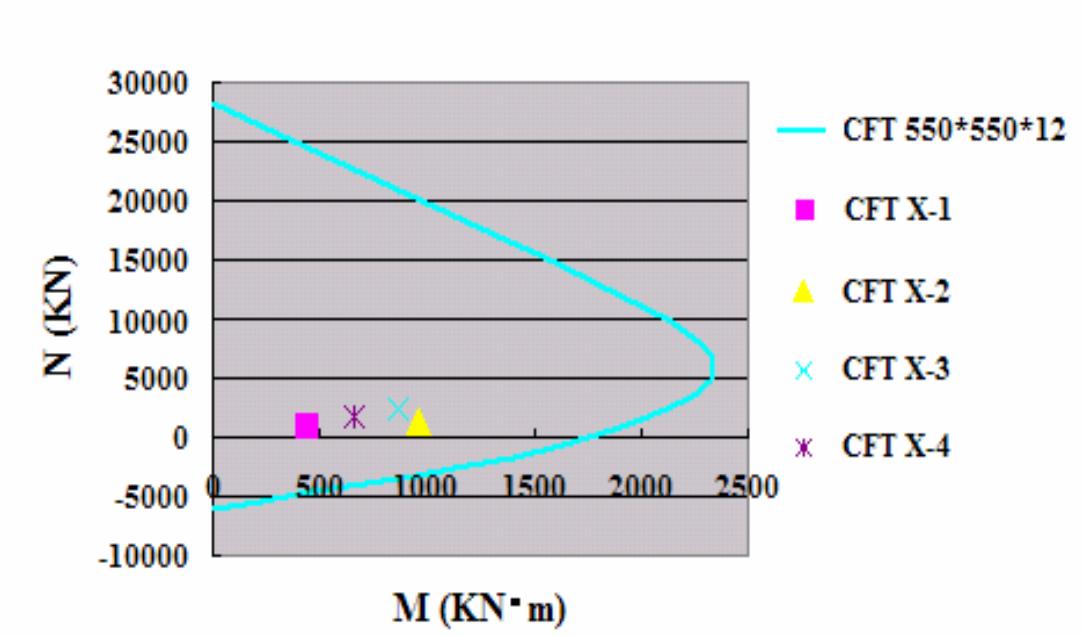

(a)

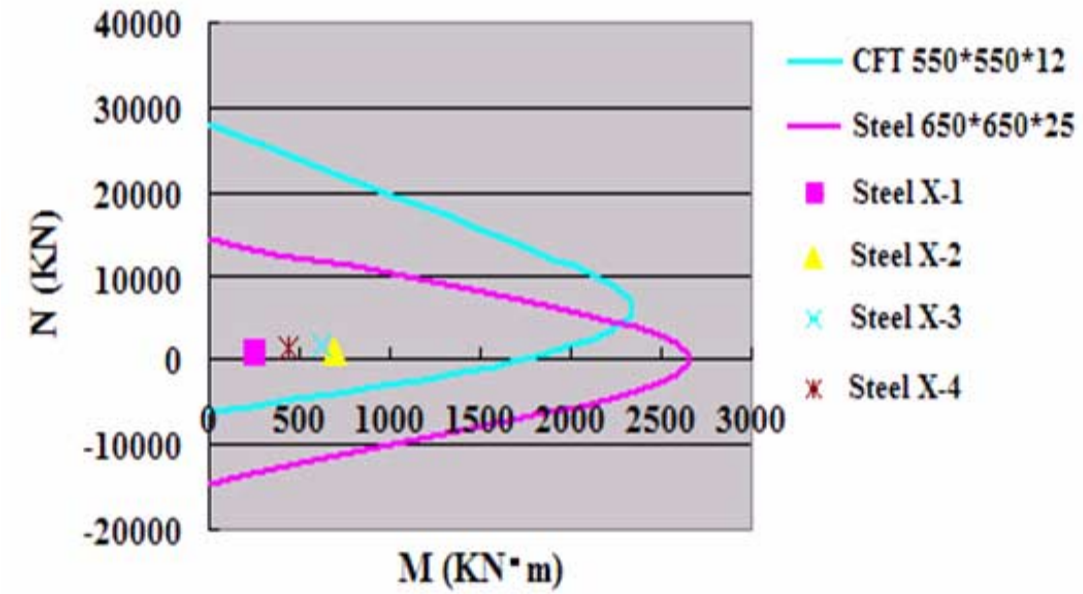

(b)

Fig 5.8 M-N Relationship of Column Member in Story 9 of 18-story Building X -direction

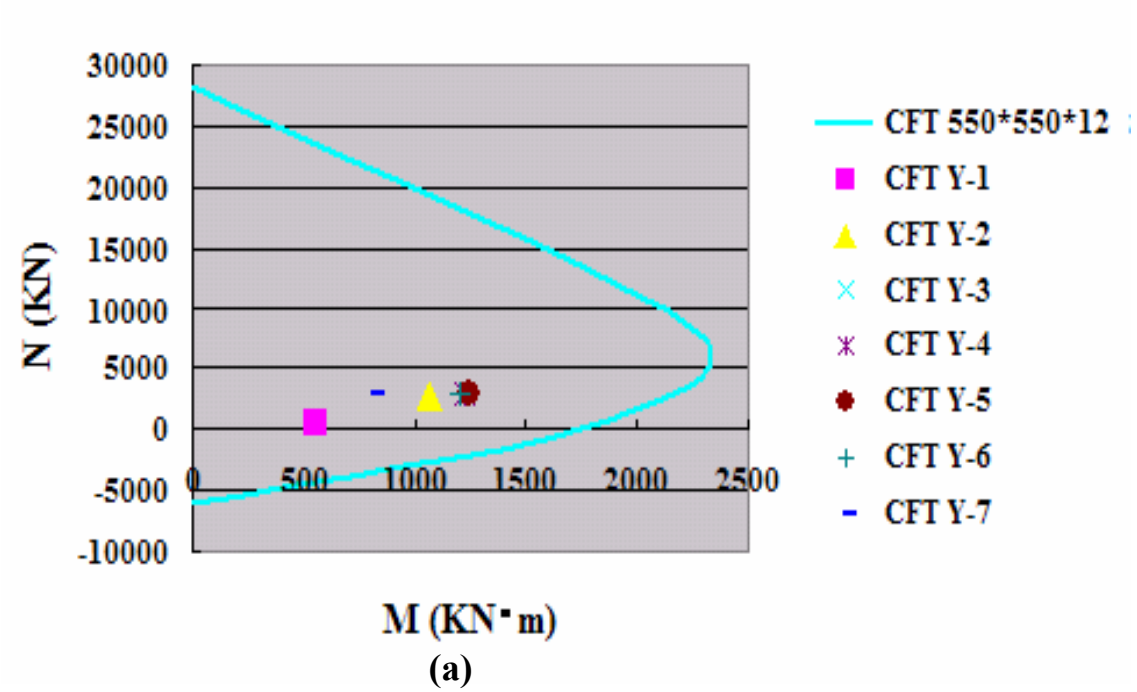

(a)

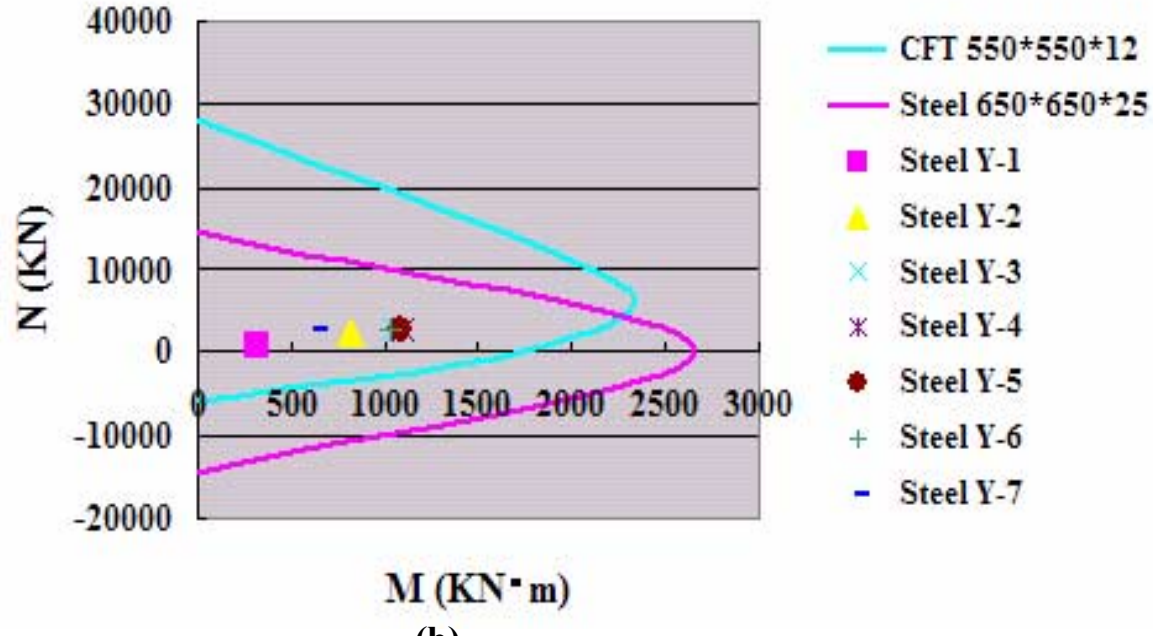

(b)

Fig 5.9 M-N Relationship of Column Member in Story 9 of 18-story Building Y -direction

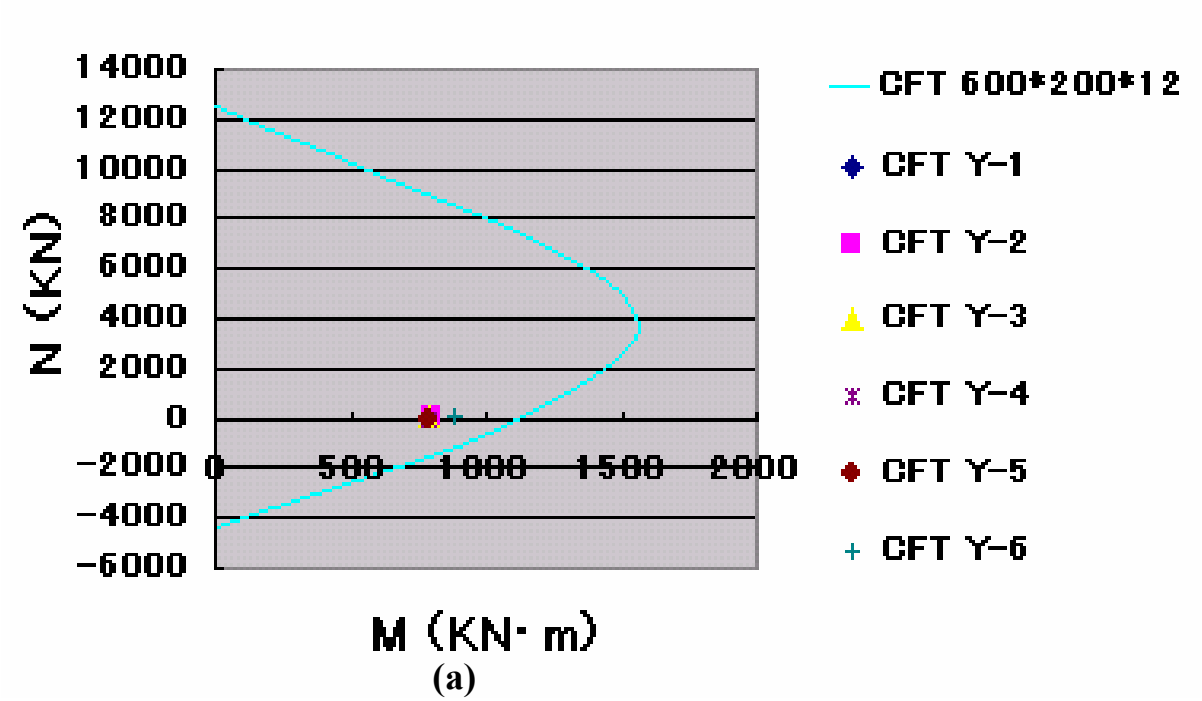

(a)

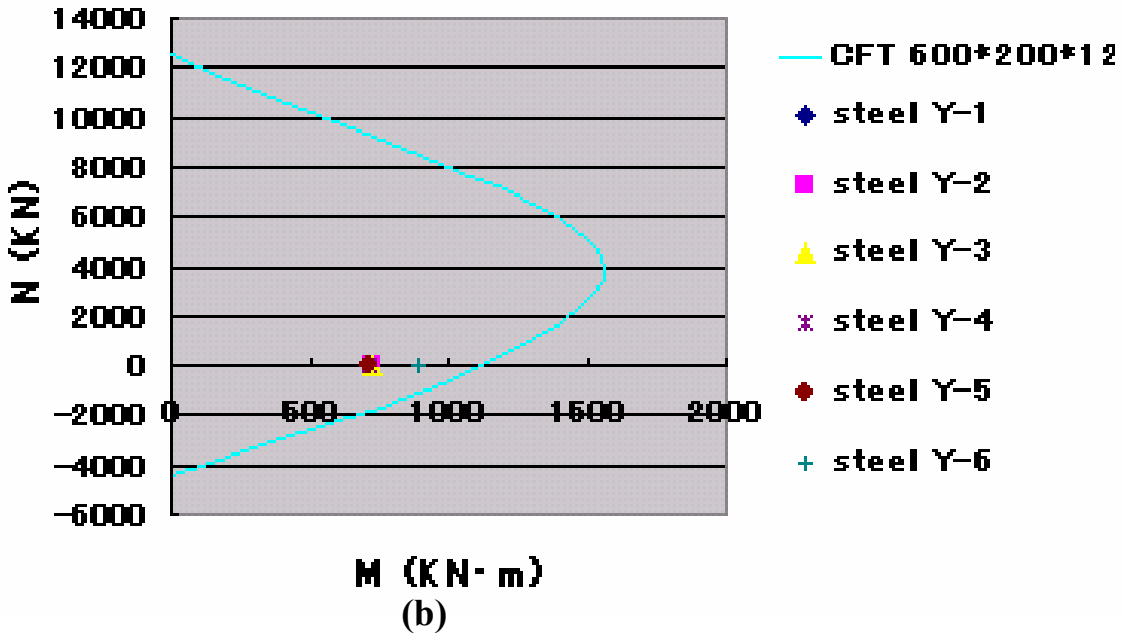

(b)

Fig 5.10 M-N Relationship of Beam Member in Story 4 of 18-story Building Y-direction

Table 5.5 shows the list of column members for 18-story building frame both in steel structure and CFT structure. The list of beam members both in steel structure and CFT structure is shown as Table 5.6.

Table5.5 Column Members List of Steel and CFT Structure of 18-story Building

	Steel structure			CFT structure		
Story	**Dimension (mm)**	**M_u (kN·m)**	**A_s (cm^2)**	**Dimension (mm)**	**M_u (kN·m)**	**A_s (cm^2)**
17-18	□-300×300×9	224	105	□-250×250×6	223	59
15-16	□-300×300×19	381	214	□-300×300×12	479	138
13-14	□-450×450×25	1138	425	□-400×400×12	889	186
11-12	□-450×450×28	1212	473	□-500×500×12	1431	234
9-10	□-650×650×25	2654	625	□-550×550×12	1750	258
7-8	□-700×700×22	2799	597	□-600×600×12	2100	282
4-6	□-750×750×19	2943	556	□-650×650×12	2483	306
1-3	□-750×750×22	3355	641	□-700×700×12	2898	330

Table5.6 Beam Members List of Steel and CFT Structure of 18-story Building

	Steel structure			CFT structure		
Story	**Dimension (mm)**	**M_u (kN·m)**	**A_s (cm^2)**	**Dimension (mm)**	**M_u (kN·m)**	**A_s (cm^2)**
17-18	H-466×199×8	283	83	□-350×150×9	327	87
15-16	H-450×200×9	344	95	□-450×200×6	406	77
13-14	H-390×300×10	457	133	□-450×200×6	406	77
11-12	H-606×201×12	685	150	□-500×200×6	486	83
9-10	H-582×300×12	799	169	□-600×200×6	695	95
1-8	H-700×300×13	1323	232	□-600×200×12	1198	186
17-18	H-450×200×9	344	95	□-350×150×9	327	87
15-16	H-390×300×10	457	133	□-450×150×9	504	105
13-14	H-606×201×12	685	150	□-550×200×6	573	89
11-12	H-582×300×12	799	169	□-550×200×9	810	132
9-10	H-692×300×13	1141	208	□-600×200×9	942	141
1-8	H-890×299×15	1790	267	□-850×250×9	1898	195

The comparison between the steel structure members and CFT structure members indicated that for column members, the areas of steel tubes of CFT columns are approximately 41~64% of that steel structure. Whereas, the yield moment of steel column members are approximately 67~130% of that steel column members. In the case of beam members, the areas of steel tubes of CFT beams are approximately 55~100% of that steel structure and the yield moment of steel beam members are approximately 71~118% of that steel beam members.

Table 5.7 shows the story drift angles values of CFT column-CFT beam frame structure and steel frame structure under design combined seismic load of the 18-story building frame. All the story drift angle values of the design building are within 1/200. The comparison result of two kinds of structure shows that all story drift angle values of CFT column-CFT beam frame structure are smaller than steel structure, which confirmed again that despite increase the dead weight, the employment of CFT structure to the beam is able to increase the stiffness of the whole structure.

5.2.7 Building frame design of 40-story office building

In order to investigate the advantage of the new CFT column-CFT beam frame structure in super high-rise building, a 40-story office building frame were designed. The design and checking method is same as 9-story and 18-story office building designs described above. Fig5.11 is the example to show checking the column members in story 17 of the 40-story building along X-direction. Fig5.12 is the example to show checking the column members in story 33 of the 18-story building along Y-direction. One example to show checking the beam members in story 17 of the 18-story building along Y-direction is shown as Fig5.13.

Table 5.8 shows the list of column members for 40-story building frame both in steel structure and CFT structure. The list of beam members both in steel structure and CFT structure is shown as Table 5.9.

The comparison between the steel structure members and CFT structure members indicated that for column members, the areas of steel tubes of CFT columns are approximately 38~68% of that steel structure. Whereas, the yield moment of steel column members are approximately 53~114% of that steel column members. In the case of beam members, the areas of steel tubes of CFT beams are approximately 70~89% of that steel structure and the yield moment of steel beam members are approximately 82~127% of that steel beam members.

Table 5.10 shows the story drift angle values of CFT column-CFT beam frame structure and steel frame structure under design combined seismic load of the 40-story building

frame. All the story drift angle values of the design building are within 1/200. The comparison result of two kinds of structure shows that all story drift angle values of CFT column-CFT beam frame structure are smaller than steel structure, which confirmed again that despite increase the dead weight, the employment of CFT structure to the beam is able to increase the stiffness of the whole structure in super high-rise building. .

Table5.7 Story Drift Angle of Steel and CFT Structure of 18-story Building under Seismic Load

Story	CFT		S		CFT/S	
	X	Y	X	Y	X	Y
18	1/260	1/269	1/259	1/264	0.996	0.981
17	1/252	1/262	1/250	1/257	0.992	0.981
16	1/248	1/262	1/245	1/255	0.988	0.973
15	1/245	1/264	1/242	1/257	0.988	0.973
14	1/249	1/273	1/245	1/263	0.984	0.963
13	1/253	1/273	1/246	1/260	0.972	0.952
12	1/261	1/278	1/246	1/260	0.943	0.935
11	1/270	1/282	1/245	1/264	0.907	0.936
10	1/280	1/289	1/247	1/271	0.882	0.938
9	1/290	1/297	1/246	1/269	0.848	0.906
8	1/294	1/300	1/244	1/266	0.830	0.887
7	1/289	1/294	1/240	1/259	0.830	0.881
6	1/284	1/290	1/236	1/254	0.831	0.876
5	1/281	1/285	1/235	1/250	0.836	0.877
4	1/282	1/284	1/239	1/249	0.848	0.877
3	1/282	1/291	1/251	1/255	0.854	0.876
2	1/323	1/307	1/283	1/270	0.876	0.879
1	1/426	1/373	1/388	1/329	0.911	0.882

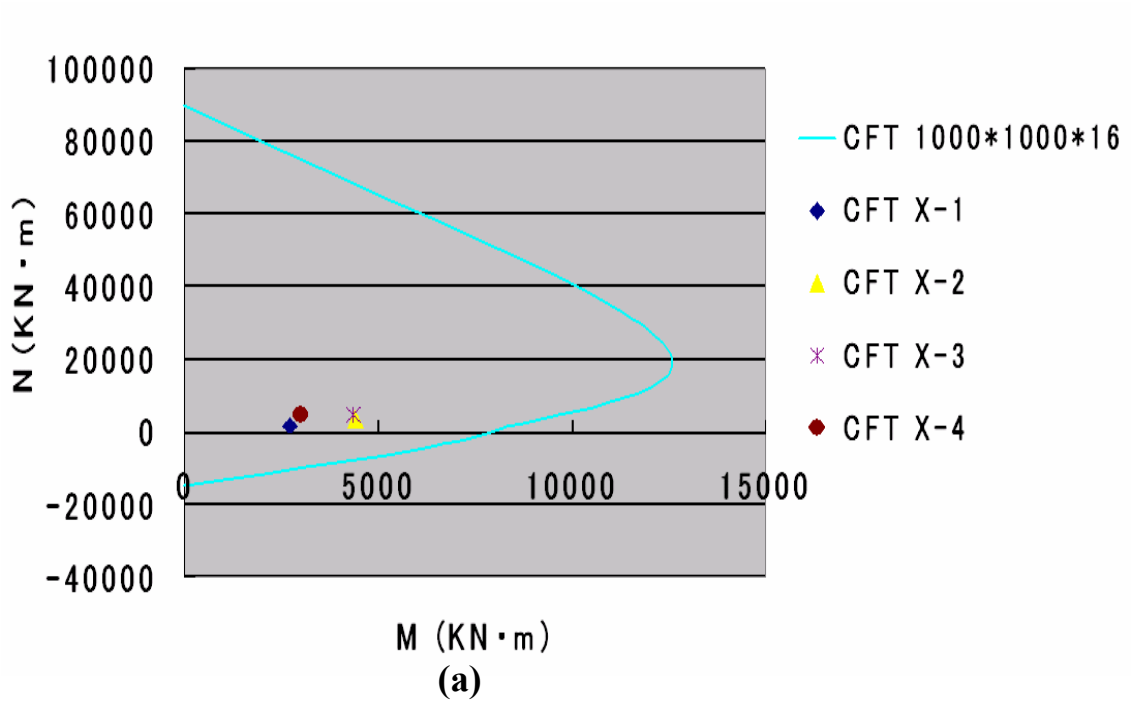

(a)

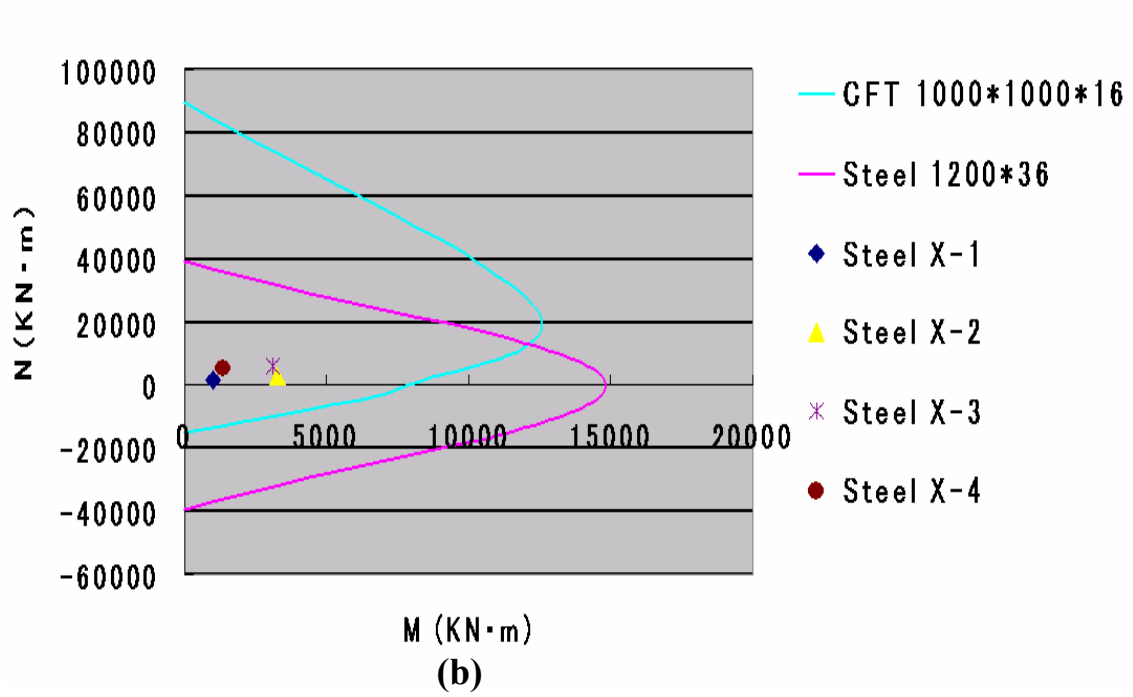

(b)

Fig 5.11 M-N Relationship of Column Member in Story 17 of 40-story Building X -direction

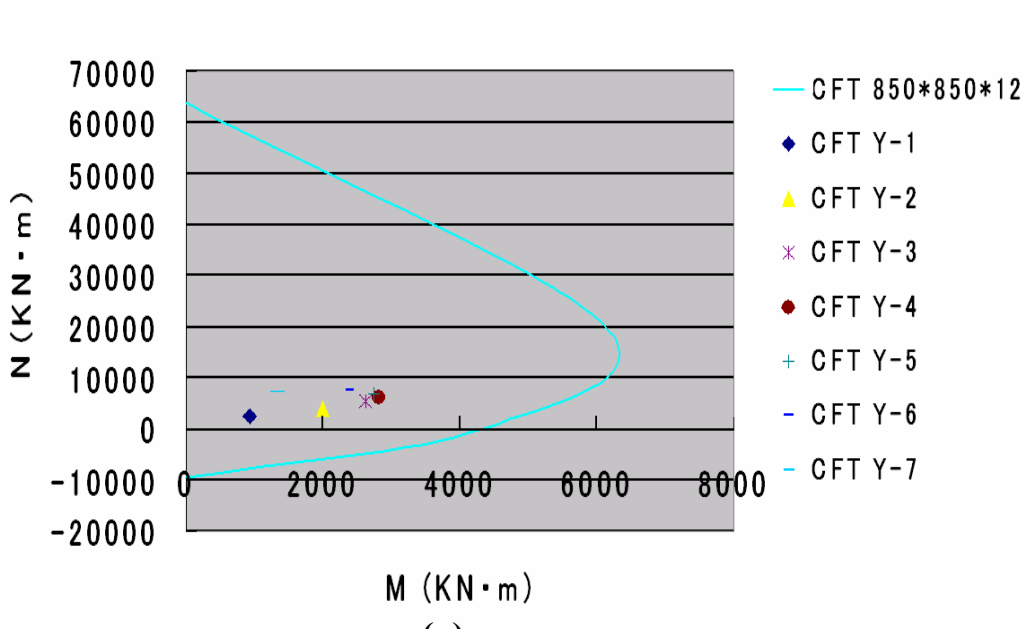

(a)

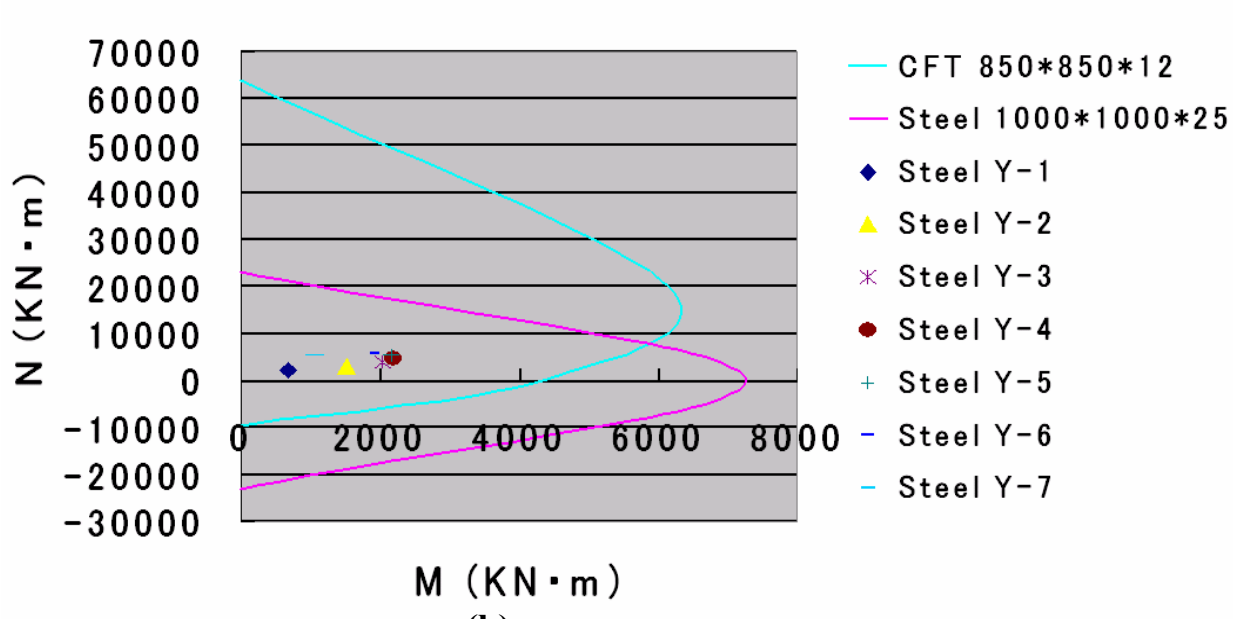

(b)

Fig 5.12 M-N Relationship of Column Member in Story 33 of 40-story Building Y -direction

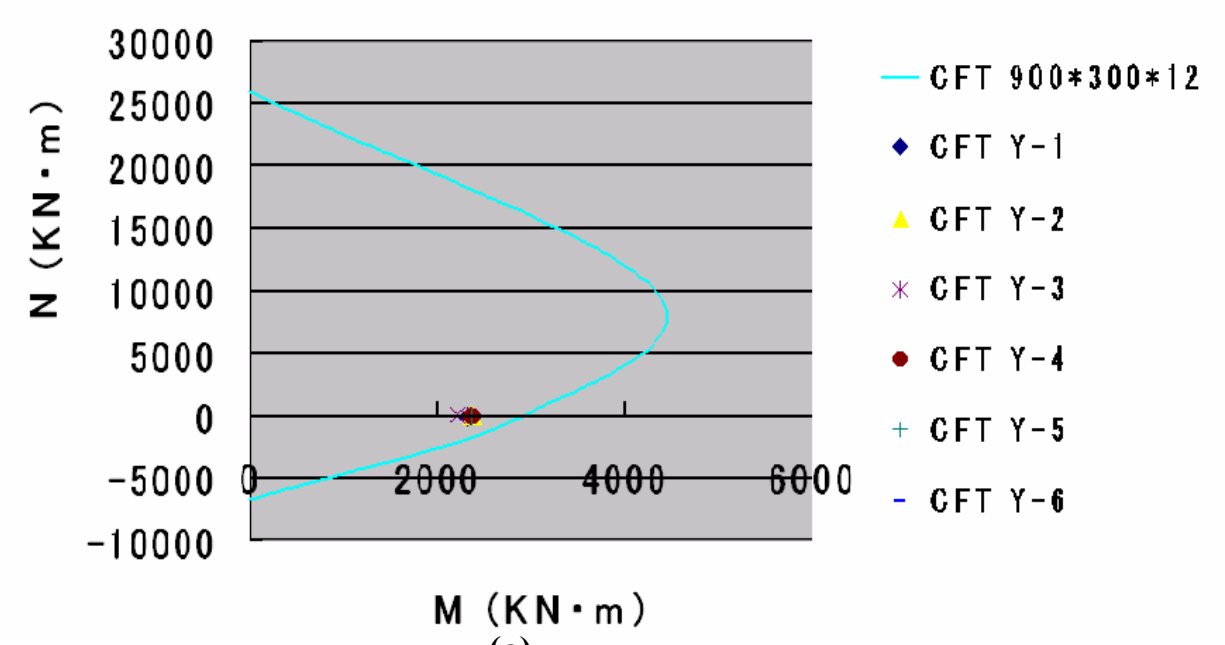

(a)

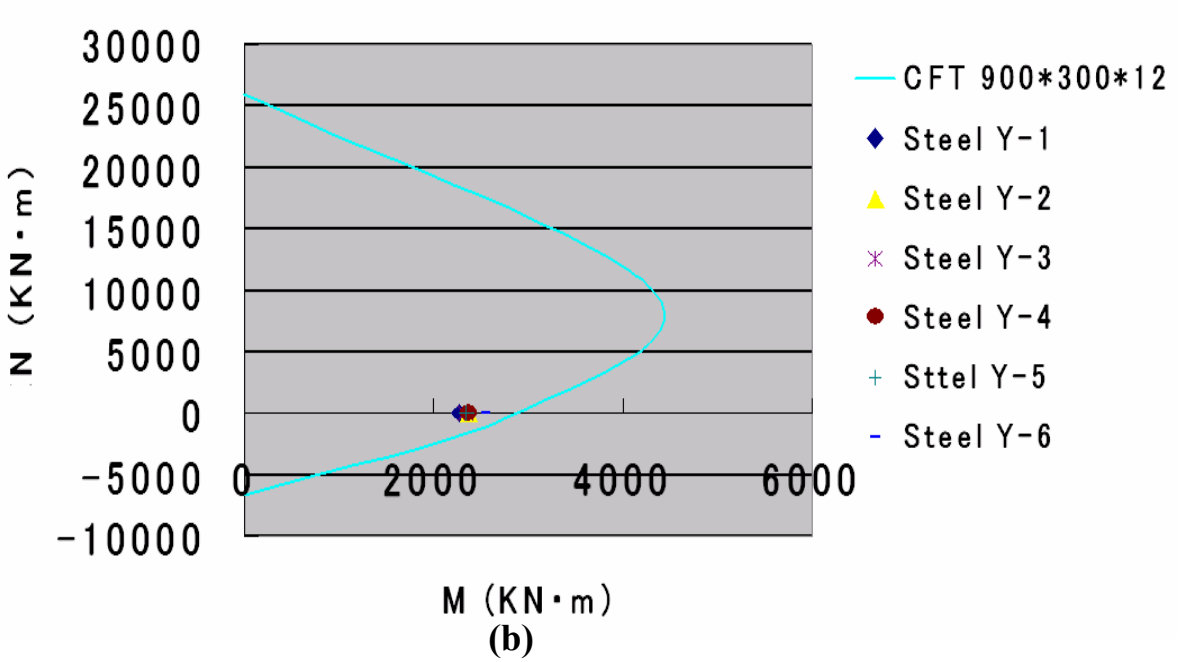

(b)

Fig5.13 M-N Relationship of Beam Member in Story 17 of 40-story Building Y-direction

Table5.8 Column Members List of Steel and CFT Structure of 40-story Building

	Steel structure			CFT structure		
Story	**Dimension (mm)**	**M_u (kN·m)**	**A_s (cm^2)**	**Dimension (mm)**	**M_u (kN·m)**	**A_s (cm^2)**
33-40	□-1000×1000×25	7265	975	□-850×850×12	4337	402
25-32	□-1100×1100×32	11114	1367	□-900×900×16	6368	566
17-24	□-1200×1200×36	14839	1676	□-1000×1000×16	7929	630
9-16	□-1200×1200×60	23276	2736	□-1200×1200×30	20519	1404
1-8	□-1300×1300×90	38642	4356	□-1300×1300×60	44080	2976

Table5.9 Beam Members List of Steel and CFT Structure of 40-story Building

	Steel structure			CFT structure		
Story	**Dimension (mm)**	**M_u (kN·m)**	**A_s (cm^2)**	**Dimension (mm)**	**M_u (kN·m)**	**A_s (cm^2)**
33-40	H-594×302×14	1060	217	□-500×200×12	874	162
25-32	H-700×300×13	1323	232	□-600×200×12	1198	186
17-24	H-900×300×16	2110	306	□-900×250×12	2687	270
9-16	H-912×302×18	2530	360	□-900×300×12	2890	282
1-8	H-900×350×16	2852	421	□-950×300×12	3176	294
33-40	H-700×300×13	1323	232	□-600×200×12	1198	186
25-32	H-800×300×14	1680	264	□-750×250×12	1949	234
17-24	H-918×303×19	2739	387	□-900×300×12	2890	282
9-16	H-900×350×16	2853	421	□-950×300×12	3176	294
1-8	H-900×400×40	3476	451	□-950×300×16	3176	390

Table5.10 Story Drift Angles of Steel and CFT Structure of 40-story Building under Seismic Load

Story	CFT		S		CFT/S	
	X	Y	X	Y	X	Y
40	1/255	1/282	1/254	1/280	0.998	0.993
39	1/253	1/278	1/250	1/276	0.987	0.993
38	1/249	1/273	1/246	1/271	0.988	0.993
37	1/245	1/269	1/242	1/266	0.989	0.999
36	1/238	1/266	1/238	1/262	0.999	0.985
35	1/236	1/262	1/235	1/258	0.997	0.985
34	1/233	1/259	1/231	1/254	0.993	0.981
33	1/230	1/257	1/229	1/251	0.995	0.977
32	1/229	1/254	1/226	1/247	0.989	0.972
31	1/228	1/251	1/224	1/244	0.983	0.972
30	1/226	1/249	1/222	1/241	0.981	0.968
29	1/225	1/246	1/220	1/238	0.977	0.967
28	1/223	1/245	1/218	1/236	0.977	0.963
27	1/223	1/243	1/217	1/234	0.973	0.963
26	1/222	1/242	1/216	1/232	0.972	0.959
25	1/222	1/241	1/215	1/230	0.967	0.954
24	1/222	1/240	1/214	1/228	0.965	0.950
23	1/222	1/238	1/212	1/225	0.953	0.945
22	1/221	1/236	1/210	1/222	0.951	0.941
21	1/221	1/234	1/208	1/220	0.943	0.940

Story	CFT		S		CFT/S	
	X	Y	X	Y	X	Y
20	1/220	1/232	1/207	1/217	0.940	0.935
19	1/219	1/231	1/206	1/215	0.941	0.931
18	1/219	1/230	1/205	1/213	0.936	0.926
17	1/218	1/230	1/204	1/211	0.934	0.917
16	1/218	1/230	1/204	1/210	0.934	0.913
15	1/219	1/229	1/204	1/209	0.933	0.913
14	1/219	1/229	1/204	1/209	0.933	0.913
13	1/219	1/229	1/204	1/209	0.933	0.913
12	1/220	1/230	1/205	1/210	0.933	0.913
11	1/222	1/231	1/207	1/212	0.932	0.918
10	1/225	1/234	1/210	1/214	0.933	0.915
9	1/230	1/239	1/215	1/219	0.934	0.916
8	1/236	1/244	1/221	1/224	0.936	0.918
7	1/245	1/251	1/229	1/230	0.936	0.916
6	1/259	1/260	1/242	1/239	0.934	0.919
5	1/277	1/274	1/260	1/253	0.937	0.923
4	1/306	1/296	1/288	1/276	0.940	0.932
3	1/357	1/337	1/337	1/315	0.944	0.935
2	1/461	1/421	1/436	1/396	0.946	0.941
1	1/756	1/662	1/714	1/622	0.944	0.940

5.3 Cost Performance Investigation

Cost performance comparison of CFT column-CFT beam frame structure and steel structure was done based on the building frame design in the former research program.

Firstly, the amount of consumed steel and concrete material of CFT column-CFT beam frame structure and steel structure was calculated, and then the cost of each building frame was estimated.

The cost estimation is based on Japanese price. Unit cost of steel is 73,060 per ton including cost of material, transportation and fabrication fees; unit cost of concrete is 28,060 per cubic meters including cost of material, transportation and construction fees as following shows:

Cost for steel	
(material & transit)	65,300 (yen/t)
+ Cost for steel fabrication	7,760 (yen/t)
Cost for steel	73,060 (yen/t)

Cost for concrete	
(material & transit)	21,000 (yen/m3)
+ Cost for concrete casting	580 (yen/m3)
Cost for concrete	21,580 (yen/t)

Cost for weld:

Weld in building site	770	(yen/m)
Weld in factory	370	(yen/m)

The amount of consumed steel and concrete material in column members and beam members of 9-story building frame was calculated respectively. Cost performance of CFT structure in column members and beam members was investigated and compared subsequently. Table5.11 and Table5.12 show the comparison result. The higher cost performance capability of CFT column which relatives to CFT beam is obviously revealed.

Cost estimation of main frames including columns, beams, weld and PC bar are shown in Table5.13. The result shows that CFT structure exhibit cost merits compared with pure steel structure.

The amount of consumed steel and concrete material in column members and beam members of 18-story and 40-story building frame was calculated respectively in the same way as 9-story building frame. Table5.14 and Table5.15 show the comparison result of consumed material and cost performance of CFT structure in column members

and beam members of 18-story building frame respectively. Table5.17 and Table5.18 show the comparison result of consumed material and cost performance of CFT structure in column members and beam members of 40-story building frame respectively. The higher cost performance capability of CFT column which relatives to CFT beam is obviously revealed as well.
Table5.16 and Table5.19 shows the comparison result of cost estimation of main frames including columns, beams, weld and PC bar of 18-story and 40-story building frame respectively. The result again confirms that CFT structure exhibit cost merits compared with pure steel structure both in high-rise building and super high-rise building.

5.4 Conclusions

According to the research work in this part of research program, the following conclusions were revealed:

1). According to the design of middle high, high-rise and super high-rise building frame, it was found that the story drift angle of new CFT column-CFT beam frame structure is close to steel structure or smaller than steel structure, which indicated that despite increase of dead weight of the building, the employ of CFT structure in beam member is able to increase the stiffness of the whole building.

2).The cost estimation result shows that the new CFT column-CFT beam frame structure is a cost-effective structure compared with pure steel structure. The building frame cost for the new CFT column-CFT beam frame structure system would be lower by approximately 10% than that of the pure steel structure system.

3).The available space of CFT column-CFT beam frame structure is able to be increased due to the decrease of dimensions of column and beam members compared with steel structure.

Table5.11 Consumed Material & Cost of Column of 9-story Building Frame

	Steel weight (t)	Steel Cost (yen)	Concrete weight (t)	Concrete volume (m^3)	Concrete cost (yen)	Total cost of column (yen)
CFT	144.850	10,582,741	283.2	118	2,546,440	13,129,181
Steel	221.439	16,178,333	--------	--------	--------	16,178,333
CFT/S	0.65	0.65	--------	--------	--------	**0.81**

Table5.12 Consumed Material & Cost of Beam of 9-story Building Frame

	Steel weight (t)	Steel Cost (yen)	Concrete weight (t)	Concrete volume (m^3)	Concrete cost (yen)	Total cost of beam (yen)
CFT	307.1	22,436,726	677.69	282.37	6,093,545	28,530,271
Steel	447.55	32,698,003	--------	--------	--------	32,698,003
CFT/S	0.69	0.69	--------	--------	--------	**0.87**

Table5.13 Cost Comparison of the 9-story CFT& Steel Structure Building frame

	CFT		S		CFT/S	
	Weight (t)	**Cost (yen)**	**Weight (t)**	**Cost (yen)**	**Weight (t)**	**Cost (yen)**
Steel	451.95	33,019,467	668.99	48,876,336	0.68	0.68
concrete	960.89	8,639,985	-------	-------	------	-------
Steel & concrete	1412.84	41,659,452	668.99	48,876,336	2.11	0.85
weld	**Weld length (m)**	**Weld cost (yen)**	**Weld length (m)**	**Weld cost (yen)**	**Weld length (m)**	**Weld cost (yen)**
	1356.4	505,198	9576.4	3,765,080	0.143	0.134
PC bar	**Weight (t)**	**Cost (yen)**	**Weight (t)**	**Cost (yen)**	**Weight (t)**	**Cost (yen)**
	10.82	2,603,704	-------	-------	------	-------
Sum		44,760,369		52,641,416		**0.85**

Table5.14 Consumed Material & Cost of Column of 18-story Building Frame

	Steel weight (t)	Steel Cost (yen)	Concrete weight (t)	Concrete volume (m^3)	Concrete cost (yen)	Total cost of column (yen)
CFT	334.02	24,403,418	1231.78	513.24	11,075,719	35,479,137
Steel	706.63	51,626,034	--------	--------	--------	51,626,034
CFT/S	0.47	0.47	--------	--------	--------	**0.67**

Table5.15 Consumed Material & Cost of Beam of 18-story Building Frame

	Steel weight (t)	Steel Cost (yen)	Concrete weight (t)	Concrete volume (m^3)	Concrete cost (yen)	Total cost of beam (yen)
CFT	658.92	48,139,270	1897.92	790.80	17,065,464	65,204,734
Steel	899.63	65,726,646	--------	--------	--------	65,726,646
CFT/S	0.73	0.73	--------	--------	--------	**0.99**

Table5.16 Cost Comparison of the 18-story CFT& Steel Structure Building frame

	CFT		S		CFT/S	
	Weight (t)	**Cost (yen)**	**Weight (t)**	**Cost (yen)**	**Weight (t)**	**Cost (yen)**
Steel	993.12	72,542,688	1606.26	117,352,680	0.62	0.62
concrete	3129.70	28,141,183	-------	-------	------	-------
Steel & concrete	4122.82	100,683,871	1606.26	117,352,680	2.57	0.86
weld	**Weld length (m)**	**Weld cost (yen)**	**Weld length (m)**	**Weld cost (yen)**	**Weld length (m)**	**Weld cost (yen)**
	2757.61	1,020,312	14715.46	7,473,890	0.187	0.137
PC bar	**Weight (t)**	**Cost (yen)**	**Weight (t)**	**Cost (yen)**	**Weight (t)**	**Cost (yen)**
	20.46	4,947,037.6	-------	-------	------	-------
Sum		106,665,879		124,826,570		**0.85**

Table5.17 Consumed Material & Cost of Column of 40-story Building Frame

	Steel weight (t)	Steel Cost (yen)	Concrete weight (t)	Concrete volume (m^3)	Concrete cost (yen)	Total cost of column (yen)
CFT	3968.85	289,964,186	10346.62	4311.09	93,033,322	382,997,508
Steel	7376.46	538,924,295	--------	--------	--------	538,924,295
CFT/S	0.54	0.54	--------	--------	--------	**0.71**

Table5.18 Consumed Material & Cost of Beam of 40-story Building Frame

	Steel weight (t)	Steel Cost (yen)	Concrete weight (t)	Concrete volume (m^3)	Concrete cost (yen)	Total cost of beam (yen)
CFT	2728.71	199,359,630	6149.97	2562.49	55,298,534	254,658,164
Steel	3491.47	255,086,887	--------	--------	--------	255,086,887
CFT/S	0.78	0.78	--------	--------	--------	**1.00**

Table5.19 Cost Comparison of the 40-story CFT& Steel Structure Building frame

	CFT		**S**		**CFT/S**	
	Weight (t)	**Cost (yen)**	**Weight (t)**	**Cost (yen)**	**Weight (t)**	**Cost (yen)**
Steel	6697.56	489,323,816	10867.93	794,011,182	0.62	0.62
concrete	16496.59	148,331,856	-------	-------	------	-------
Steel & concrete	23194.15	637,655,672	10867.93	794,011,182	2.13	0.80
weld	**Weld length (m)**	**Weld cost (yen)**	**Weld length (m)**	**Weld cost (yen)**	**Weld length (m)**	**Weld cost (yen)**
	14615.28	5,407,654	73577.30	37,369,450	0.199	0.145
PC bar	**Weight (t)**	**Cost (yen)**	**Weight (t)**	**Cost (yen)**	**Weight (t)**	**Cost (yen)**
	116.62	28,198,111	-------	-------	------	-------
Sum		671,261,355		831,380,632		**0.81**

CHAPTER 6

CONCLUSIONS AND RECOMMENDATIONS

6.1 Summary

Concrete-filled steel Tube (CFT) structure has many advantages over ordinary steel or reinforced concrete structure. Combination of steel and concrete in one member results in a member that has the beneficial qualities of both materials. Although CFT column steel beam frame system has gained popularity in building construction, the CFT structure has not been employed in beam member, thus no CFT column-CFT beam frame system has been applied to building construction until now.

From the viewpoint of application of this new CFT system, design and select a suitable connection detail used between the CFT column and CFT beam with sufficient seismic behavior and low cost are essential. Different connection details were designed in this research work. In order to assess the strength and ductility of the different connection detail, three CFT column-CFT beam subassemblies with different connection details were made and tested. The test specimen represented column and beam in an intermediate story and was subjected to a constant axial load and a cyclic lateral load. The information gained from this experimental study was used to identify the suitable connection detail for the new proposed CFT structure. Moreover, one hollow steel tube column-H beam subassembly also was made and tested in order to compare with the proposed CFT column-CFT beam structure. Based on the review of previous studies, it was concluded that the PC bar linked connection detail is a more appropriate connection detail to achieve the sufficient strength, stiffness, and ductility than other details.

This research also proposed a new bottom up pumping method which was developed basing on the existing bottom up pumping method for CFT column system. Firstly, the idea and feasibility of this idea were analysed in the research. Parts of mortar in concrete will attach on the inner surface of the steel tube during the flowing period. This will lead to coarse aggregate concentrate to the forepart of concrete flow; thus segregation may occur after concrete flows through horizontal beam to the adjacent column and drops from top to the bottom of the column. In order to further investigate the amount of these attached mortars, experiment on investigation of thickness of mortar which adheres to steel plate surface was subsequently conducted in a steel

trough using fresh concrete. The experimental result revealed that segregation may not occur due to few amount of mortar attaching on the inner surface of steel tube.

Visual model of fresh concrete experimental work was conducted in this research in order to further investigate the flow tendency of concrete in the real building. A scale subassembly which was made of acrylics plate was made and visual model of fresh concrete was poured inside the subassembly in order to simulate the real flow tendency of concrete in the steel tubes of column and beam. In the two experiment projects, concrete with superior properties and inferior properties were simulated by the visual model respectively. The experimental result showed that visual model which simulated superior concrete can be successfully constructed into the column-beam subassembly. This result indicated that the proposed bottom up pumping method for the new CFT column-CFT beam frame system is feasible. Whereas, the visual model which simulated inferior concrete experimental result showed that block will easily occur during the construction period due to the inferior properties of concrete leading to the segregation between mortar and coarse aggregate.

Besides the advantages of employ CFT structure in beam such as improve the stiffness of whole building, delay the local buckling of beam and improve fireproof performance of the whole building, the new proposed CFT column-CFT beam frame system should has advantage in cost performance. The cost performance was investigated basing on building frame design of different story buildings both using CFT column-CFT beam frame system and pure steel frame system in this research.

6.2 Conclusions

6.2.1 Experimental Research on Seismic Behavior of New CFT Column-CFT Beam frame Structure

1) The experiment result shows that self-compacting concrete (SCC) can be successfully compacted into beam tube, which indicates that CFT column-CFT beam frame can be made using SCC.

2) The substantial deformation capacity expected was obtainable in two PC bar jointed CFT column-CFT beam connection specimens. Insufficient thickness of PC bar flange led to a little larger deformation of PC bar flange. Increase of the thickness is inferred able to strengthen the connection.

6.2.2 Construction Method for New CFT Column-CFT Beam Frame Structure

3) Concrete can be poured through several input ports only made on several columns and more than one story frame can be constructed using the new developed bottom up pumping method. The employ of branch pipe in this construction method also can decrease the number of pump car. Therefore, compared with the existed bottom up pumping method for CFT column-Steel frame structure, the new construction method for the new CFT column-CFT beam frame structure is supposed to be an efficient and cost-effective method.

4) Experiment on thickness of mortar which adheres to steel plate surface simulated the concrete flow in beam. The experiment result reveals the fact that the property of concrete changed during the concrete flow period. Mortar volume ratio changed due to amount of mortar adhering to the steel plate surface until it arrived to the value of original design and kept stable.
   The thickness of mortar which adhered to the steel plate surface is around 1.4mm to1.5mm.

6.2.3 Investigation of the New Developed Bottom up Pumping Method Using Visual Model of Fresh Concrete

2) The proposed new developed bottom up pumping method for the new CFT column-CFT beam frame structure in chapter 3 can be simulated by the visual model of fresh concrete. The flow tendency of concrete in column-beam subassembly is able to be observed obviously. The proposed construction method is supposed to be feasible to be applied on condition that the fresh concrete has prior properties.

2) The experimental work also revealed that block may easily occur due to the inferior properties of fresh concrete. The compaction quality will be strongly affected due to the segregation occurrence between coarse aggregate and mortar. Pouring speed also effect the construction result. Lower pouring speed led to earlier occurrence of block than higher pouring speed.

6.2.4 Building Frame Design and Cost Performance analysis

1). According to the design of middle high, high-rise and super high-rise building frame, it was found that the story drift angle of new CFT column-CFT beam frame structure is close to steel structure or smaller than steel structure, which indicated that despite increase of dead weight of the building, the employ of CFT structure in beam member is able to increase the stiffness of the whole building.

2). The cost estimation result shows that the new CFT column-CFT beam frame structure is a cost-effective structure compared with pure steel structure. The building frame cost for the new CFT column-CFT beam frame structure system would be lower by approximately 10% than that of the pure steel structure system.

3).The available space of CFT column-CFT beam frame structure is able to be increased due to the decrease of dimensions of column and beam members compared with steel structure.

From review of the whole research work which had been done in this research, it indicated that the proposed new CFT column-CFT beam frame structure is a kind of cost-effective, construction-convenient, high-performance structure. The proposed bottom up pumping method is supposed to provide an efficient construction method for the new CFT structure. Concrete flow simulation experiment using visual model intuitively verified the feasibility of the proposed construction method. The new CFT system is inferred able to be applied in building construction industry in the future.

6.3 Recommendations for Future Research

The new CFT column-CFT beam frame structure is firstly proposed in this research. Although many issues related to connection detail design and comparison, seismic behavior investigation, construction method proposition and cost performance estimation had been conducted in this research work, many further research works are still need to be done in this field. The following is a list of suggested areas where additional research is needed.

1) Only two kinds of connection details for the new proposed CFT column-CFT beam structure were designed and compared in this research work. Between these two kinds of connection details, PC bar linked connection detail was identified more superior than Outer-diaphragm connection detail not only in seismic behavior but

also in construction advantage. In the future research work, more connection details should be designed and compared in order to further identify a more suitable connection detail for the proposed new CFT column-CFT beam frame structure. Besides the high seismic behavior, the more suitable connection detail should be constructed conveniently by the fabricators as well as lead to economy of composite construction.

Additional testing on specimens with different connection details is required to study in order to more fully understand the behavior of the different connection details, basing on which the more suitable connection detail is decided.

2) A developed bottom up pumping method which based on the existed construction method for CFT column system was proposed in this research. In order to investigate the concrete flow tendency in the steel tube, visual model of fresh concrete was employed in the concrete construction simulation experimental work. The successful construction and good compacting quality of concrete with superior properties as well as block occurrence and bad distribution of mortar and coarse aggregate in tubes due to the segregation of concrete with inferior properties were able to be easily observed by visual model simulation experimental work. However, the visual model is unable to accurately simulate the fresh concrete qualitatively.

   In order to more accurately understand the real situation of concrete construction in the building site, more experimental work which can simulate the real situation more closely by employing fresh concrete should be done in the future research work. Thus the proposed construction method for the new CFT column-CFT beam frame structure can be further assured to be practiced.

3) Comparison of CFT column-CFT beam frame structure and pure steel structure based on trial designs showed that the new proposed CFT structure can increase the stiffness of the whole building, the total steel consumption of the new proposed CFT structure system is less than that of the pure steel structure system, which lead to more advantageous for the new proposed CFT structure in cost performance than pure steel structure. However, these trial designs had been done only in the case of that both of the structures were applied to unbraced frames. It is needed to investigate the performance of other type of structural systems, such as the combination of the new CFT system with reinforced-concrete structural shear wall, which may provide more merit.

References

1. AIJ Standards for Structural Calculation of Steel Reinforced Concrete Structures. Architectural Institute of Japan (AIJ), 1987.

2. Specification for Structural Steel Design. Architectural Institute of Japan (AIJ), 1986.

3. Limit State Design of Steel Frames. Architectural Institute of Japan (AIJ), 2002.

4. Recommendation for Limit State Design of Steel Structures. Architectural Institute of Japan (AIJ), 1998

5. Design Standard for Steel Structures. Architectural Institute of Japan (AIJ), 1973

6. Recommendations for Loads on Buildings. Architectural Institute of Japan (AIJ), 1993 revision.

7.Cost of Architectural Construction Material. Cost of Architectural Construction Material Association of Japan. 1999 Aug.

8. Zhong Shantong, The Concrete-Filled Steel Tubular Structures. Qinghua University Publishing Company, Beijing, 2003

9. Recommendations for Design and Construction of Concrete Filled Steel Tubular Structures. Association of New Urban Housing Technology, 2002.

10. Elremaily, A. and Azizinamini, A. "Experimental behavior of steel beam to CFT column connections". Journal of Constructional Steel Research, 2001; 57(10), 1099-1119.

11. Elremaily, A. and Azizinamini, A. "Design Provisions for Connections Between Steel Beams and Concrete Filled Tube Columns" Journal of Constructional Steel Research, 2001; 57(10), 971-995.

12. Morino, S., Uchikoshi, M. and Yamaguchi, I. "Concrete-Filled Steel Tube Column System-Its Advantages ". Steel Structures, 2001; (1) 33-44.

13. Morino, S. and Tsuda, K. " Design and Construction of Concrete-Filled Steel Tube Columnn System in Japan". Earthquake Engineering and Engineering Seismology, 2002;4 (1) 51-73

14. Beutel, J., Thambiratnam, D. and Perera, N. "Cyclic behaviour of concrete filled steel tubular column to steel beam connections". Engineering Structures, 2002; 24(1), 29-38.

15. Kato, B., Kimura, M., Ohta, H and Mizutani, N. "Connection of Beam Flange to Concrete-filled Tubular Column". Composite Construction in Steel and Concrete, 1992 June 528-538.

16.Chiew, S. P., Lie, S.T. and Dai, Ch. W. "Moment resistance of steel I-beam to CFT Column Connections". Journal of Structural Engineering, 2001; 127(10), 1164-1172.

17. Soh, C.K., Chiew, S. P., and Dong, Y.X. "Damage Model for Concrete-steel Interface". Journal of Engineering Mechanics, 1999; Aug. 979-983.

18. Kawaguchi, J., Ueda, M. and Morino, S. "Elasto-Plastic Behavior of Concrete Filled Steel Tubular Frames". Journal of Constructional Steel, 2, 25-32.

19. Kanatani, H., Tabuchi, M., Kamba, T., Hsiaolien, J. and Ishikawa, M. "A Study on Concrete Filled RHS Column to H-Beam Connections Fabricated with HT Bolts in Rigid frames". Composite Construction in Steel and Concrete, 1987, June, 614-635.

20. Morita, K., Yokoyama, Y., Kawamata, Y. and Matsumura, H. "Effect of Inner Ring Stiffer on the Strength of Connection Between Steel Beam and Concrete-filled Square tube Column". Journal of Structural and Construction Engineering, Transactions of AIJ, 1991, 422, 85-96.

21. Hajjar, J. F. and Gourley, B.C. "Representation of Concrete-Filled Steel Tube Cross-Section Strength". Journal of Structural Engineering, 1996,122(11), 1327-1336.

22. Dogan, E. and Krstulovic, N. " Seismic Retrofit with Continuous Slurry-Infiltrated Mat Concrete Jackets". ACI Structural Journal, 2003 100(6) 713-722.

23. Okamura, H., Ozawa, K. and Ouchi, M. "Self-compacting Concrete". Structural Concrete, 2000; 1(1), 3-17.

24.Okamura, H., and Ouchi, M. "Self-compacting Concrete". Journal of Advanced Concrete Technology, 2003; 1(1) 5-15.

25. Bartos, P.J.M and Cechura, J. "Improvement of working environment in Concrete Construction by the use of Self-compacting Concrete". 2001; 2(3) 127-132.

26. Recommendation for Self-compacting Concrete. Japan Society of Civil Engineers (JSCE) 1999.

27. Chang, S., Chung, J. Kimura, J., and Matsui, C. "Experimental Study of New Structural System of H-shaped Beam-to-Square Column Connection with Outer Diaphragm ". Steel Construction Engineering, 2002, 34(9), 9-15.

28. Cheng, B. "Constructional Feature of Steel-pipe Concrete Column and Steel Structure of Shenzhen Saiger Plaza". Construction Technology, 2000, 6(29) 2-5.

29.Zhao, J. and Zhang, F. "Pumping Concrete through Tubular Bottom- Construction Technology of Concrete Filled Steel Tubular Column" Architecture Technology, 2001, 32(2) 89-90.

30.Wu, J., Li, J. and Song, M. "Construction Technology o f Concrete Filled Steel Tubular Column in Project of Telecommunication Business Building of Jiangsu Province". Architecture Technology, 2001,32(2) 91-92.

31. Zhang, F. "Construction Technique of Steel Tubular Concrete Columns in Xingye Building of Guangzhou". Building Technique Development, 2003, 30(2), 75-76.

32. Hashimoto, O. "Development of Visual Model of Fresh Concrete ". PHD Thesis, Nagaoka University of Technology, Nagaoka, Japan.

Acknowledgement

I would like to thank my adviser, Professor Shima Hiroshi, for his guidance and support through the progress of this research. His vast expertise made this work possible. I would also like to acknowledge President Okamura Hajime for giving good advice for this research. Thanks extend to other members of the supervisory committee for their helpful suggestions.

Suggestions provide by professor Fujisawa Nobumitsu and Ouchi Masahiro, are greatly appreciated. I would also like to thank Mr. Miyaj for his help during the experimental phase of the project. Thanks also go to my fellow graduate students Mr. Chalermchai Wattanalamlerd, Mr. Han Virak, Mr. Vong Seng for their help and support.

The research was conducted under the close collaboration of all members in concrete structure laboratory of Kochi University of Technology. The authors are grateful to all Master students and undergraduate students for their help during the phase of experimental work.

I would like to thank my family and friends for their moral support during the course of my graduate studies. Finally, my deepest gratitude goes to my parents for their love, support, encouragement, patience, and understanding.

Wang Ying
Kochi University of Technology
Dec. 2005